phenomenon that the ability to form G418-resistant colonies depends on persistent expression of neomycin phosphotransferase from replicating HCV RNAs. siHCV decreased the formed G418-resistant colonies by 99.6%.

The 5′ untranslated region (UTR) and the upstream portion of the core region are the most conserved parts in the HCV genome, with an nt identity of 99.6% (211,212). Therefore, the 5′ UTR appears to be an ideal target for siRNA. Yokota et al. (213) investigated the effect of siRNA targeting the 5′ UTR on HCV IRES-mediated translation, HCV replication, and protein expression. siRNA decreased luciferase activity by 81% at a concentration of only 2.5 nM in Huh7 cells transiently transfected with an HCV IRS reporter gene vector. This vector expresses mRNA consisting of the HCV 5′ UTR and the upstream part of the core region, connected in-frame with the firefly luciferase (FL) gene as reporter. siRNA decreased luciferase activity, the non-structural viral proteins NS3, -4, and -5, and intracellular replication of HCV genome RNA in Huh7 cells stably expressing an HCV Feo replicon that expressed mRNA consisting of FL and NS3, -4, -5A, and -5B.

The high degree of sequence diversity between different HCV genotypes and the notoriously error-prone replication of HCV are the major problems in the development of siRNA-based gene therapies.

Kronke et al. (214) developed two alternative strategies to overcome these obstacles. In one approach, they used endoribonuclease-prepared siRNAs (esiRNAs) to simultaneously target multiple sites of the HCV genome and investigated the effect of esiRNAs on the replication of subgenomic and genomic HCV replicon in Huh cells transfected with HCV replicon encoding FL as a reporter. siRNAs directed against various regions of the HCV coding sequence as well as the 5′ UTR efficiently inhibited reporter gene expression to $\approx 1\%$. siRNAs also reduced the number of subgenomic replicon RNAs to $\approx 1\%$. In an alternative approach, pseudotyped retroviruses encoding shRNA were generated. A retroviral vector expressing shRNA targeting domain IV or nearby coding sequences inhibited reporter gene expression in Huh cells.

Takigawa et al. (215) utilized two methods to express shRNAs: one utilizing an expression plasmid and the other utilizing a recombinant lentivirus vector. The efficacy of a number of shRNAs directed against different target regions of the HCV genome in Huh cells transfected with HCV subgenomic replicon was determined. In both systems, shRNAs against NS3-1 (nucleotides 2052–2060) and NS5B (nucleotides 7326–7344) most efficiently suppressed expression of NS3 protein and reduced the amount of HCV replicon RNA.

The proteasome α-subunit PSMA7 modulates HCV-IRES activity in cell culture (216). The Hu antigen R (HuR) is a member of the ELAV-like protein family (217), which binds to HCV 3′ UTR RNA sequences (218).

Korf et al. (219) investigated the effect of a panel of DNA-based retroviral vectors expressing siRNAs against the highly conserved HCV-5′ and -3′ UTRs or the putative HCV cofactors PSMA7 and HuR on HCV IRES-mediated translation and subgenomic replication. siRNAs directed against highly conserved HCV-5′ and -3′ UTRs reduced HCV-IRES activity from the dual-gene luciferase reporter in Huh7 cells. These cells had been transfected with the dual-gene HCV-IRES reporter construct driven by the SV40 promoter to direct cap-dependent translation of renilla luciferase and cap-independent HCV IRES-mediated translation of FL. siRNAs inhibited HCV replicon RNA and HCV-NS5B protein expression in Huh cells harboring single-gene, subgenomic HCV replicons composed of regions such as the HCV 5′ UTR, nucleotides 342–389 of the core-encoding sequence, the HCV non-structural proteins NS3 to -5B, and the HCV 3′ UTR. siRNAs directed against PSMA7 and HuR reduced HCV-IRES activity from the dual-gene HCV-IRES reporter construct. siRNAs inhibited HCV replicon RNA and HCV-NS5B protein expression in Huh cells harboring single-gene, subgenomic HCV replicons. Selected combinations of HCV-directed siRNAs and siRNAs targeting PSMA7 and HuR or a combination of two siRNAs against these cofactors caused an additive inhibitory effect to that of subgenomic HCV replicons in Huh cells harboring single-gene, subgenomic HCV replicons.

HBV X protein induces HIV-1 replication and transcription through NF-κB binding sites in the HIV-1 long terminal repeat promoter (220). Specifically, the NS5a HCV protein activates NF-κB, in turn activating the promoter function of HIV-LTR (221,222).

Strayer et al. (223) exploited these findings to illustrate the potential applicability of such conditional expression approaches to drive the transcription of siRNA targeting HCV mRNA. siRNA was delivered with Tag-deleted SV40-derived vectors containing HIV-1 LTR. siRNA reduced the HCV-NS5A mRNA level by >98% in HepG2 cells stably expressing the HCV full genome. Specificity was confirmed by the finding that the siRNA delivered with the SV40-derived vector containing mutated HIV-1 LTR had no effect on the mRNA level.

Hamazaki et al. (224) synthesized shRNAs targeting the HCV IRES core gene transcript using T7 RNA polymerase and investigated the effect of shRNAs on the replication of HCV RNA in an HCV replicon stably expressing the HCV subgenome. shRNAs inhibited HCV replication by >90%. shRNAs did not induce luciferase activity in Huh7 cells or an HCV replicon transfected with a luciferase reporter gene-expressing vector with IFN-regulatory factor-3 binding regions. shRNAs did not induce IFN-β and did not activate PKR or 2′,5′-OAS in Huh7 cells and HCV replicon. These findings indicate that the shRNAs inhibit replication of HCV RNA without inducing an IFN response.

Inhibition of HBV gene expression and replication by RNAi

HBV is an enveloped virus with a partially ds relaxed-circular 3.2-kb DNA genome encoding polymerase, X protein, core antigen (C), and surface (PreS and S) (Fig. 2). With an estimated 400 million chronic carriers worldwide, HBV infection remains one of the most prevalent chronic viral infections in humans (225). Chronic infections have serious consequences, including cirrhosis and HCC (226), and are responsible for >1 million deaths annually (225). Current treatments for chronic HBV are suboptimal. Nucleoside or nt analogs, such as lamivudine and adefovir dipivoxil, suppress HBV replication effectively (227,228), but suffer from the selection of drug-resistant mutations and a high rate of relapse when treatment is discontinued (229). Although IFN-α and pegylated IFN-α have both immunomodulatory and antiviral effects, they achieve a sustained response in only a small percentage of patients and are usually associated with a wide array of side-effects (230,231). Thus, alternative therapeutic approaches for chronic HBV are needed. A number of groups have attempted to verify the usefulness of RNAi as a therapeutic tool in several model systems, as described below. The findings indicate that siRNA and shRNA against HBV efficiently interfere with HBV gene expression and replication.

McCaffrey et al. (232) investigated the effect of U6 shRNAs targeting C and S regions on the production of HBV intermediates in Huh7 cells, plus immunocompetent and immunodeficient mice transfected with a plasmid containing the HBV genome with some sequences duplicated to allow complete expression of all genes. shRNA reduced the amounts of HBsAg in culture medium and mouse serum by 94.2% and 84.5%, respectively. Immunohistochemistry indicated that shRNA reduced HBV core antigen (HBcAg) by >99%. Immunocompetent and immunocompromised mice treated with shRNA had 77% and 92% less HBV RNA, respectively. shRNA reduced HBV ss and ds DNA-replicative intermediates to undetectable levels.

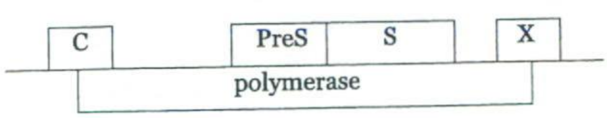

Fig. 2. Schematic representation of the HBV genome.

Giladi et al. (233) investigated the effect of siRNA targeting HBsAg on HBV gene expression and replication in both HepG2.2.215 cells transfected with HBV plasmid and in mice transfected with HBV plasmid. In their systems, injection of Balb/c mice with the HBV genomic plasmid resulted in the production and secretion of HBV-related antigens and replicative intermediates into the serum for >1 week. By 10 days, viral particle production subsides, concomitant with the appearance of anti-HBV antibodies. siRNA reduced the amount of HBsAg and HBV nucleocapsid antigen (HBeAg) in culture media by >80%. siRNA reduced HBV 3.6-kb and 2.1/2.4-kb mRNA species, and also reduced the amounts of HBsAg and HBeAg in mouse serum by 90% and 80%, respectively. Immunohistochemistry indicated that the siRNA diminished HBsAg-positive cells by >0.1%. siRNA reduced the three species of mRNAs by ≈50%. siRNA diminished HBV DNA in serum by >100-fold.

Konishi et al. (234) investigated the effect of siRNA targeting to polyadenylation (PA), precore (Prec), and S regions on replication of HBV in HepG2.2.215 cells transfected with HBV plasmid. HBsAg secretion into culture media was inhibited by 78%, 67%, and 42% with siRNAs against the PA, PreC, and S regions, respectively. siRNA against the PA region decreased levels of HBV pre-genomic RNA and HBV RNA containing the PA signal sequence by 72% and 86%, respectively. siRNA decreased the level of HBV core-associated DNA, a replication intermediate, by 71%. Immunohistochemistry indicated that siRNA decreased HBsAg-positive cells by 30–40%.

Shlomai and Shaul (235) investigated the effect of siRNA-producing vectors targeting the C and X ORF regions at the level of HBV proteins, transcripts, and HBV replicative forms in Huh and HepG2.2.15 cells. siRNAs against X and C regions significantly decreased levels of X and C proteins in Huh7 cells transfected with X and C region plasmids, respectively. siRNA against the X region significantly decreased the number of green fluorescent protein-positive cells in Huh7 cells transfected with HBV-GFP plasmid, in which the C region was replaced with GFP. siRNA against the X region decreased core protein in HepG2.2.15 cells stably expressing HBV. siRNA against the X region decreased levels of all viral transcripts and viral replicative intermediates by ≈68% and ≈95%, respectively in Huh7 cells transfected with 1.3 X HBV genome plasmid. siRNA against the C region decreased levels of all viral transcripts and viral replicative intermediates by ≈13% and 40%, respectively in the Huh7 cells transfected with 1.3 X HBV genome plasmid.

Hamasaki et al. (236) investigated the effect of shRNA targeting to the core region on replication of HBV in Huh7 and HepG2 cells transfected with HBV genome plasmid. shRNA decreased the amount of HBeAg in culture media by 4.6- and 4.9-fold in Huh and HepG2 cells, respectively. shRNA decreased 3.5-kb mRNA of HBV plus the viral replicative intermediates, open circular and ss HBV-DNA in Huh cells.

Ying et al. (237) investigated the effect of siRNA targeting of the C region on viral replication in HepAD38 cells (producing wild-type virus) and HepAD59 cells (producing 3TC-resistant YMDD variant). siRNA inhibited viral DNA synthesis by 98% and 89% in HepAD38 cells and HepAD59 cells, respectively. siRNA decreased HBV core protein synthesis in HepAD38 cells, in which HBV replication was induced by removal of tetracycline from the culture medium.

Klein et al. (238) developed a novel mouse model to study HBV replication and investigated the effect of siRNA targeting of the ORFs of the S and C regions on expression of HBsAg and HBeAg using this model. In this model it is possible to introduce a replication-competent vector into hepatocytes and to activate HBV replication by a high-volume injection via the tail vein using an HBV replication-competent vector. siRNA targeting to the ORF of the S region decreased HBsAg and HBeAg in the serum by nearly 70% and 80%, respectively. siRNA decreased pre-C/C and S RNA levels in the liver. siRNA targeting to the ORF of the C region located outside the S region decreased HBeAg protein in serum and mRNA levels in the liver by 60% and 74%, respectively, whereas siRNA had no effect on the HBsAg protein level.

Chen et al. (239) investigated U6 shRNAs targeting different putative secondary structures on HBV pregenomic RNA, HBV RNA, and HBV replication in HepG2 cells transfected with HBV plasmids. Targeted sequences included direct repeat elements or regions coding for C, PreS, S, polymerase, and X protein. shRNAs decreased HBV RNA and the relative copy number of HBV DNA by up to 90% and by 90–97%, respectively.

Wu et al. (240) investigated the effect of plasmid-expressing siRNA targeting HBV C region nucleotides 2052–2070 on the replication and expression of HBV in mice transfected with HBV plasmid containing a 1.3-fold-overlength genome of HBV. siRNA decreased serum HBsAg and HBV C mRNA levels on Day 6 by ≈90% and 85%, respectively. Immunohistochemistry indicated that siRNA decreased HBcAg-positive cells from 5.4% to 0.9%.

Morrissey et al. (241) introduced some chemical modifications to siRNAs to improve their stability and investigated the effect of targeting siRNAs to the HBV genome in a mouse and a HepG2 cell model of HBV replication. The combination of modifications included 2′-fluoro, 2′-*O*-methyl, and 2′-deoxy sugars, phosphorothionate linkage, and terminus capping chemistries, plus complete removal of 2′-OH. The modified siRNA duplex prolonged the half-life ≈900-fold compared with the unmodified siRNA duplexes in 90% human serum at 37°C. The modified siRNA targeting a site located at starting 5′ nt 263 in the HBV genome decreased HBsAg in the culture media by ≈80% in HepG2 cells transfected with replication-competent HBV expression plasmid. The 263 siRNA decreased the HBV RNA level by 71% in mice transfected with complete HBV genome vector. The 263 siRNA and unmodified siRNA decreased serum HBV DNA by $10^{-3.7}$ and $10^{-2.2}$ at a dose of 1 μg. Similar results were obtained for serum HBsAg levels. When the 263 siRNA was delivered 3 days after transfection of the HBV vector it decreased serum HBV DNA levels by $10^{-0.9}$.

The same group (242) also synthesized stable nucleic acid–lipid particle (SNALP) formulations of stabilized siRNA, investigating its efficacy using several criteria. Stabilized siRNA-SNALP almost completely eliminated HBsAg protein in culture media of HepG2 cells transfected with HBV plasmid with an IC_{50} of −1 nM. Stabilized siRNA-SNALP prolonged the half-life in plasma to approximately eightfold compared to stabilized siRNA in mice. Non-stabilized siRNA-SNALP strongly induced serum IFN-α or inflammatory cytokines (IL-6, TNF-α), plus serum aspartate aminotransferase and alanine aminotransferase, whereas such effects were not observed in the stabilized siRNA-SNALP. Stabilized siRNA-SNALP reduced serum HBV DNA by $>10^{-1.0}$ in a mouse model of HBV replication. The reduction in HBV DNA was dose-dependent and lasted for up to 6 weeks. Furthermore, reductions were seen in serum HBV DNA for up to 6 weeks with weekly dosing.

Uprichard et al. (243) investigated the effect of Ad vector expressing U6 RNA polymerase III-driven shRNAs targeting HBV regions overlapping 3.5-, 2.4-, and 2.1-kb RNA on preexisting HBV gene expression and replication in HBV transgenic mice. The HBV-specific siRNA numbers, HBV 546 and HBV 765, refer to the initial nt of siRNA relative to the unique viral EcoRI site. shRNAs decreased the amount of HBsAg and HBeAg in serum by five- to sixfold on Day 4. The reduction in HBsAg and HBeAg levels continued until 13 days. shRNAs decreased the 2.1-kb envelope and 3.5-kb viral RNA in the liver by >50-fold and by four- to fivefold on Day 20, respectively. The same authors also did similar experiments using HBV transgenic mice that are genetically deficient for the expression of IFN-γ and the IFN-α/β receptor, as in vivo Ad does induce IFNs that clear HBV DNA from the liver. HBV 765 decreased HBsAg and HBeAg on Day 26 by ≈20-fold and 10-fold, respectively. HBV 765 decreased 2.1- and 3.5-kb RNA on Days 17–26 to an undetectable level and by 10-fold, respectively. This pattern of HBV RNA inhibition was maintained through to Day 26. HBV 765 decreased HBV replicative intermediate to virtually undetectable levels on Days 17–26. Immunohistochemistry indicated that HBV 765 decreased HBcAg-positive cells in the liver to an undetectable level on Days 17 and 26.

Wu et al. (244) investigated the effect of the human H1 promoter-encoded shRNAs targeting the S regions on the viral proteins, RNA, and DNA for three HBV genotypes in several models. shRNA decreased HBsAg and HBeAg protein in the culture media on Days 6 and 2 by 98.2% and 62.6%, respectively in Huh7 cells transfected with HBV genotype A plasmid. shRNA markedly decreased HBV RNA in cells and HBV replicative DNA in culture media and the cytoplasm. shRNA decreased HBsAg in the serum by >99% on Day 4 in mice transfected with HBV genotype A plasmid. Immunohistochemistry indicated that shRNA decreased HBcAg-positive cells in the liver by >95%. shRNA also decreased HBsAg and HBeAg in the culture media by ≈95% and 85%, respectively in Huh7 cells transfected with HBV genotype B or C plasmids. In these experiments, a clone from a patient with genotype C was resistant to shRNA. This mutant clone was found to exhibit a silent mutation in the target regions and could be selected out in the presence of shRNA in cell culture.

Carmona et al. (245) investigated the effect of a panel of shRNAs targeting the HBx ORF region on HBV replication in several models. To facilitate intracellular processing, the shRNAs included mismatches in the 25-bp stem region and a terminal loop of micro RNA-23. Two shRNAs (−5 and −6) decreased HBsAg secretion and HBV–GFP fusion marker protein without inducing IFN responses by >95% and ≈60% in Huh7 cells transfected with HBV plasmid and HBV–GFP fusion plasmid, respectively. The two shRNAs did not affect IFN response: induction of IFN-β, OAS1, and MxA in Huh7 cells. shRNAs decreased HBV RNA to ≈35% in Huh7 cells transfected with HBV plasmid. shRNA5 decreased HBsAg in serum to a background level over a period of 4 days in HBV transgenic mice. Immunohistochemistry indicated that shRNA5 decreased HBcAg-positive cells in the liver to an almost undetectable level. The two shRNAs decreased HBsAg and viral particle concentration in serum by >99% on Day 4 in mice. Carmona et al. incorporated the two shRNAs into an Ad vector to assess the antiviral efficacy of these shRNAs in a context similar to that of natural HBV infection. The two Ad vector shRNAs decreased HBsAg and HBeAg in serum by >90% and ≈50% by Day 12. Ad shRNAs −5 and −6 decreased the virion count in serum by 60% and 98% in mice, respectively.

Kim et al. (246) investigated the effect of siRNA and U6 shRNAs targeting positions 1374–1392 of the HBx sequence on the HBx mRNA level in HepG2-HBX expressing HBx mRNA and HepG2-K8 producing HBV particle. siRNA and tU6 shRNA reduced the HBx mRNA level by up to 80–90% in these cells. They also investigated the effect of siRNA and U6 shRNA on GFP expression in HepG2 cells transfected with HBx–eGFP fusion plasmid. siRNA and U6 shRNA reduced GFP expression by 90%. Chromosomal integration of U6 shRNA into HepG2 cells was also confirmed.

Chen et al. (247) investigated the effect of a ds adeno-associated virus eight-pseudotyped vector expressing shRNA targeting the S1 region of HBV on levels of HBV protein, mRNA, and replicative DNA in HBV transgenic mice. This shRNA decreased HBsAg protein and HBV genome in serum by >99% at 14 days. shRNA decreased 2.4/2.1- and 3.5-kb HBV transcripts by 93% and 81%, respectively. shRNA almost completely eliminated HBV replicative intermediates, intrahepatic relaxed-circular, and ss linear viral DNA. Immunohistochemistry indicated that shRNA almost completely eliminated HBcAg-positive cells in the liver. These reductions persisted for >120 days. Reductions in HBsAg, HBV DNA, and HBV replicative intermediates at 120 days were 66.1%, 77.1%, and 75.8%, respectively. shRNA induced only negligible amounts of IFN-γ and -β, and 2′,5′-OAS.

Acknowledgements

This work was supported by a Grant-in-Aid for Cancer Research (No. 15-2) from the Ministry of Health, Labor and Welfare of Japan.

References

1. Hannon GJ. RNA interference. Nature 2002;418:244–51.
2. McManus MT, Petersen CP, Haines BB, Chen J, Sharp PA. Gene silencing using micro-RNA designed hairpins. RNA 2002;8:842–50.
3. Hammond SM, Caudy AA, Hannon GJ. Post-transcriptional gene silencing by double-stranded RNA. Nat Rev Genet 2001;2:110–9.
4. Zamore PD. RNA interference: listening to the sound of silence. Nat Struct Biol 2001;8:746–50.
5. Hamilton AJ, Baulcombe DC. A species of small antisense RNA in posttranscriptional gene silencing in plants. Science 1999;286:950–2.
6. Hammond SM, Bernstein E, Beach D, Hannon GJ. An RNA-directed nuclease mediates post-transcriptional gene silencing in Drosophila cells. Nature 2000;404:293–6.
7. Zamore PD, Tuschl T, Sharp PA, Bartel DP. RNAi: double-stranded RNA directs the ATP-dependent cleavage of mRNA at 21 to 23 nucleotide intervals. Cell 2000;101:25–33.
8. Elbashir SM, Lendeckel W, Tuschl T. RNA interference is mediated by 21- and 22-nucleotide RNAs. Genes Dev 2001; 15:188–200.
9. Bernstein E, Caudy AA, Hammond SM, Hannon GJ. Role for a bidentate ribonuclease in the initiation step of RNA interference. Nature 2001;409:363–6.
10. Yang D, Lu H, Erickson JW. Evidence that processed small dsRNAs may mediate sequence-specific mRNA degradation during RNAi in Drosophila embryos. Curr Biol 2000;10: 1191–200.
11. Elbashir SM, Harborth J, Lendeckel W, Yalcin A, Weber K, Tuschl T. Duplexes of 21-nucleotide RNAs mediate RNA interference in cultured mammalian cells. Nature 2001;411: 494–8.
12. Stark GR, Kerr IM, Williams BR, Silverman RH, Schreiber RD. How cells respond to interferons. Annu Rev Biochem 1998;67:227–64.
13. Samuel CE. Antiviral actions of interferons. Clin Microbiol Rev 2001;14:778–809.
14. Yu JY, DeRuiter SL, Turner DL. RNA interference by expression of short-interfering RNAs and hairpin RNAs in mammalian cells. Proc Natl Acad Sci U S A 2002;99:6047–52.
15. Sui G, Soohoo C, Affar el B, Gay F, Shi Y, Forrester WC, et al. A DNA vector-based RNAi technology to suppress gene expression in mammalian cells. Proc Natl Acad Sci U S A 2002;99:5515–20.
16. Miyagishi M, Taira K. U6 promoter-driven siRNAs with four uridine 3′ overhangs efficiently suppress targeted gene expression in mammalian cells. Nat Biotechnol 2002;20: 497–500.
17. Paul CP, Good PD, Winer I, Engelke DR. Effective expression of small interfering RNA in human cells. Nat Biotechnol 2002;20:505–8.
18. Maeda I, Kohara Y, Yamamoto M, Sugimoto A. Large-scale analysis of gene function in Caenorhabditis elegans by high-throughput RNAi. Curr Biol 2001;11:171–6.
19. Waterhouse PM, Helliwell CA. Exploring plant genomes by RNA-induced gene silencing. Nat Rev Genet 2003;4:29–38.
20. Harborth J, Elbashir SM, Bechert K, Tuschl T, Weber K. Identification of essential genes in cultured mammalian cells using small interfering RNAs. J Cell Sci 2001;114: 4557–65.
21. Cottrell TR, Doering TL. Silence of the strands: RNA interference in eukaryotic pathogens. Trends Microbiol 2003;11:37–43.
22. Gitlin L, Andino R. Nucleic acid-based immune system: the antiviral potential of mammalian RNA silencing. J Virol 2003;77:7159–65.
23. Caplen NJ. RNAi as a gene therapy approach. Expert Opin Biol Ther 2003;3:575–86.
24. Li K, Lin SY, Brunicardi FC, Seu P. Use of RNA interference to target cyclin E-overexpressing hepatocellular carcinoma. Cancer Res 2003;63:3593–7.
25. Mitaka T, Sattler CA, Sattler GL, Sargent LM, Pitot HC. Multiple cell cycles occur in rat hepatocytes cultured in the presence of nicotinamide and epidermal growth factor. Hepatology 1991;13:21–30.
26. Mitaka T, Mikami M, Sattler GL, Pitot HC, Mochizuki Y. Small cell colonies appear in the primary culture of adult rat hepatocytes in the presence of nicotinamide and epidermal growth factor. Hepatology 1992;16:440–7.
27. Tateno C, Yoshizato K. Long-term cultivation of adult rat hepatocytes that undergo multiple cell divisions and express normal parenchymal phenotypes. Am J Pathol 1996;148: 383–92.
28. Tateno C, Yoshizato K. Growth and differentiation in culture of clonogenic hepatocytes that express both phenotypes of hepatocytes and biliary epithelial cells. Am J Pathol 1996;149:1593–605.
29. Niimi S, Oshizawa T, Yamaguchi T, Harashima M, Seki T, Ariga T, et al. Specific expression of annexin III in rat-small-hepatocytes. Biochem Biophys Res Commun 2003;300: 770–4.
30. Niimi S, Harashima M, Gamou M, Hyuga M, Seki T, Ariga T, et al. Expression of annexin A3 in primary cultured parenchymal rat hepatocytes and inhibition of DNA synthesis by suppression of annexin A3 expression using RNA interference. Biol Pharm Bull 2005;28:424–8.
31. Saltiel AR, Kahn CR. Insulin signalling and the regulation of glucose and lipid metabolism. Nature 2001;414:799–806.
32. Postic C, Dentin R, Girard J. Role of the liver in the control of carbohydrate and lipid homeostasis. Diabetes Metab 2004;30:398–408.
33. Chakravarty K, Cassuto H, Reshef L, Hanson RW. Factors that control the tissue-specific transcription of the gene for phosphoenolpyruvate carboxykinase-C. Crit Rev Biochem Mol Biol 2005;40:129–54.
34. Lee YH, Koh SS, Zhang X, Cheng X, Stallcup MR. Synergy among nuclear receptor coactivators: selective requirement for protein methyltransferase and acetyltransferase activities. Mol Cell Biol 2002;22:3621–32.
35. Koh SS, Chen D, Lee YH, Stallcup MR. Synergistic enhancement of nuclear receptor function by p160 coactivators and two coactivators with protein methyltransferase activities. J Biol Chem 2001;276:1089–98.
36. Krones-Herzig A, Mesaros A, Metzger D, Ziegler A, Lemke U, Bruning JC, et al. Signal-dependent control of gluconeogenic key enzyme genes through coactivator-associated arginine methyltransferase 1. J Biol Chem 2006;281:3025–9.
37. Camacho IA, Nagarkatti M, Nagarkatti PS. 2,3,7,8-Tetrachlorodibenzo-p-dioxin (TCDD) induces Fas-dependent activation-induced cell death in superantigen-primed T cells. Arch Toxicol 2002;76:570–80.

38. Cantrell SM, Joy-Schlezinger J, Stegeman JJ, Tillitt DE, Hannink M. Correlation of 2,3,7,8-tetrachlorodibenzo-p-dioxin-induced apoptotic cell death in the embryonic vasculature with embryotoxicity. Toxicol Appl Pharmacol 1998;148:24–34.
39. Christensen JG, Gonzales AJ, Cattley RC, Goldsworthy TL. Regulation of apoptosis in mouse hepatocytes and alteration of apoptosis by nongenotoxic carcinogens. Cell Growth Differ 1998;9:815–25.
40. Kamath AB, Xu H, Nagarkatti PS, Nagarkatti M. Evidence for the induction of apoptosis in thymocytes by 2,3,7,8-tetrachlorodibenzo-p-dioxin in vivo. Toxicol Appl Pharmacol 1997;142:367–77.
41. Kamath AB, Camacho I, Nagarkatti PS, Nagarkatti M. Role of Fas-Fas ligand interactions in 2,3,7,8-tetrachlorodibenzo-p-dioxin (TCDD)-induced immunotoxicity: increased resistance of thymocytes from Fas-deficient (lpr) and Fas ligand-defective (gld) mice to TCDD-induced toxicity. Toxicol Appl Pharmacol 1999;160:141–55.
42. McConkey DJ, Hartzell P, Duddy SK, Hakansson H, Orrenius S. 2,3,7,8-Tetrachlorodibenzo-p-dioxin kills immature thymocytes by Ca2+-mediated endonuclease activation. Science 1988;242:256–9.
43. Rhile MJ, Nagarkatti M, Nagarkatti PS. Role of Fas apoptosis and MHC genes in 2,3,7,8-tetrachlorodibenzo-p-dioxin (TCDD)-induced immunotoxicity of T cells. Toxicology 1996;110:153–67.
44. Sakamoto MK, Mima S, Tanimura TA. Morphological study of liver lesions in Xenopus larvae exposed to 2,3,7,8-tetrachlorodibenzo-p-dioxin (TCDD) with special reference to apoptosis of hepatocytes. J Environ Pathol Toxicol Oncol 1995;14:69–82.
45. Okey AB, Riddick DS, Harper PA. Molecular biology of the aromatic hydrocarbon (dioxin) receptor. Trends Pharmacol Sci 1994;15:226–32.
46. Schmidt JV, Su GH, Reddy JK, Simon MC, Bradfield CA. Characterization of a murine Ahr null allele: involvement of the Ah receptor in hepatic growth and development. Proc Natl Acad Sci U S A 1996;93:6731–6.
47. Park KT, Mitchell KA, Huang G, Elferink CJ. The aryl hydrocarbon receptor predisposes hepatocytes to Fas-mediated apoptosis. Mol Pharmacol 2005;67:612–22.
48. Ziegelbauer J, Shan B, Yager D, Larabell C, Hoffmann B, Tjian R. Transcription factor MIZ-1 is regulated via microtubule association. Mol Cell 2001;8:339–49.
49. Ziegelbauer J, Wei J, Tjian R. Myc-interacting protein 1 target gene profile: a link to microtubules, extracellular signal-regulated kinase, and cell growth. Proc Natl Acad Sci U S A 2004;101:458–63.
50. Lu TT, Makishima M, Repa JJ, Schoonjans K, Kerr TA, Auwerx J, et al. Molecular basis for feedback regulation of bile acid synthesis by nuclear receptors. Mol Cell 2000;6: 507–15.
51. Delerive P, Galardi CM, Bisi JE, Nicodeme E, Goodwin B. Identification of liver receptor homolog-1 as a novel regulator of apolipoprotein AI gene transcription. Mol Endocrinol 2004;18:2378–87.
52. Zanjani ED, Poster J, Burlington H, Mann LI, Wasserman LR. Liver as the primary site of erythropoietin formation in the fetus. J Lab Clin Med 1977;89:640–4.
53. Dame C, Fahnenstich H, Freitag P, Hofmann D, Abdul-Nour T, Bartmann P, et al. Erythropoietin mRNA expression in human fetal and neonatal tissue. Blood 1998;92: 3218–25.
54. Weiss MJ, Orkin SH. GATA transcription factors: key regulators of hematopoiesis. Exp Hematol 1995;23:99–107.
55. Aird WC, Parvin JD, Sharp PA, Rosenberg RD. The interaction of GATA-binding proteins and basal transcription factors with GATA box-containing core promoters. A model of tissue-specific gene expression. J Biol Chem 1994; 269:883–9.
56. Nemer G, Nemer M. Transcriptional activation of BMP-4 and regulation of mammalian organogenesis by GATA-4 and -6. Dev Biol 2003;254:131–48.
57. Cirillo LA, Lin FR, Cuesta I, Friedman D, Jarnik M, Zaret KS. Opening of compacted chromatin by early developmental transcription factors HNF3 (FoxA) and GATA-4. Mol Cell 2002;9:279–89.
58. Goldberg MA, Glass GA, Cunningham JM, Bunn HF. The regulated expression of erythropoietin by two human hepatoma cell lines. Proc Natl Acad Sci U S A 1987;84:7972–6.
59. Dame C, Sola MC, Lim KC, Leach KM, Fandrey J, Ma Y, et al. Hepatic erythropoietin gene regulation by GATA-4. J Biol Chem 2004;279:2955–61.
60. Guo S, Rena G, Cichy S, He X, Cohen P, Unterman T. Phosphorylation of serine 256 by protein kinase B disrupts transactivation by FKHR and mediates effects of insulin on insulin-like growth factor-binding protein-1 promoter activity through a conserved insulin response sequence. J Biol Chem 1999;274:17184–92.
61. Puigserver P, Rhee J, Donovan J, Walkey CJ, Yoon JC, Oriente F, et al. Insulin-regulated hepatic gluconeogenesis through FOXO1-PGC-1alpha interaction. Nature 2003; 423:550–5.
62. Schmoll D, Walker KS, Alessi DR, Grempler R, Burchell A, Guo S, et al. Regulation of glucose-6-phosphatase gene expression by protein kinase Balpha and the forkhead transcription factor FKHR. Evidence for insulin response unit-dependent and -independent effects of insulin on promoter activity. J Biol Chem 2000;275:36324–33.
63. Vander Kooi BT, Streeper RS, Svitek CA, Oeser JK, Powell DR, O'Brien RM. The three insulin response sequences in the glucose-6-phosphatase catalytic subunit gene promoter are functionally distinct. J Biol Chem 2003;278:11782–93.
64. Yeagley D, Guo S, Unterman T, Quinn PG. Gene- and activation-specific mechanisms for insulin inhibition of basal and glucocorticoid-induced insulin-like growth factor binding protein-1 and phosphoenolpyruvate carboxykinase transcription. Roles of forkhead and insulin response sequences. J Biol Chem 2001;276:33705–10.
65. Nakae J, Park BC, Accili D. Insulin stimulates phosphorylation of the forkhead transcription factor FKHR on serine 253 through a Wortmannin-sensitive pathway. J Biol Chem 1999;274:15982–5.
66. Rena G, Guo S, Cichy SC, Unterman TG, Cohen P. Phosphorylation of the transcription factor forkhead family member FKHR by protein kinase B. J Biol Chem 1999;274: 17179–83.
67. Biggs WH 3rd, Meisenhelder J, Hunter T, Cavenee WK, Arden KC. Protein kinase B/Akt-mediated phosphorylation promotes nuclear exclusion of the winged helix transcription factor FKHR1. Proc Natl Acad Sci U S A 1999;96:7421–6.
68. Matsuzaki H, Daitoku H, Hatta M, Tanaka K, Fukamizu A. Insulin-induced phosphorylation of FKHR (Foxo1) targets to proteasomal degradation. Proc Natl Acad Sci U S A 2003; 100:11285–90.
69. Rena G, Prescott AR, Guo S, Cohen P, Unterman TG. Roles of the forkhead in rhabdomyosarcoma (FKHR) phosphorylation sites in regulating 14-3-3 binding, transactivation and nuclear targetting. Biochem J 2001;354:605–12.
70. Zhang X, Gan L, Pan H, Guo S, He X, Olson ST, et al. Phosphorylation of serine 256 suppresses transactivation by

FKHR (FOXO1) by multiple mechanisms. Direct and indirect effects on nuclear/cytoplasmic shuttling and DNA binding. J Biol Chem 2002;277:45276–84.

71. Sotaniemi EA, Pelkonen O, Arranto AJ, Tapanainen P, Rautio A, Pasanen M. Diabetes and elimination of antipyrine in man: an analysis of 298 patients classified by type of diabetes, age, sex, duration of disease and liver involvement. Pharmacol Toxicol 2002;90:155–60.
72. Thummel KE, Schenkman JB. Effects of testosterone and growth hormone treatment on hepatic microsomal P450 expression in the diabetic rat. Mol Pharmacol 1990; 37:119–29.
73. Yamazoe Y, Murayama N, Shimada M, Yamauchi K, Kato R. Cytochrome P450 in livers of diabetic rats: regulation by growth hormone and insulin. Arch Biochem Biophys 1989; 268:567–75.
74. Kawamura A, Yoshida Y, Kimura N, Oda H, Kakinuma A. Phosphorylation/Dephosphorylation steps are crucial for the induction of CYP2B1 and CYP2B2 gene expression by phenobarbital. Biochem Biophys Res Commun 1999;264: 530–6.
75. Sidhu JS, Omiecinski CJ. Insulin-mediated modulation of cytochrome P450 gene induction profiles in primary rat hepatocyte cultures. J Biochem Mol Toxicol 1999;13:1–9.
76. Yoshida Y, Kimura N, Oda H, Kakinuma A. Insulin suppresses the induction of CYP2B1 and CYP2B2 gene expression by phenobarbital in adult rat cultured hepatocytes. Biochem Biophys Res Commun 1996;229:182–8.
77. Honkakoski P, Zelko I, Sueyoshi T, Negishi M. The nuclear orphan receptor CAR-retinoid X receptor heterodimer activates the phenobarbital-responsive enhancer module of the CYP2B gene. Mol Cell Biol 1998;18:5652–8.
78. Wei P, Zhang J, Egan-Hafley M, Liang S, Moore DD. The nuclear receptor CAR mediates specific xenobiotic induction of drug metabolism. Nature 2000;407:920–3.
79. Ueda A, Hamadeh HK, Webb HK, Yamamoto Y, Sueyoshi T, Afshari CA, et al. Diverse roles of the nuclear orphan receptor CAR in regulating hepatic genes in response to phenobarbital. Mol Pharmacol 2002;61:1–6.
80. Kodama S, Koike C, Negishi M, Yamamoto Y. Nuclear receptors CAR and PXR cross talk with FOXO1 to regulate genes that encode drug-metabolizing and gluconeogenic enzymes. Mol Cell Biol 2004;24:7931–40.
81. Brown MS, Goldstein JL. A receptor-mediated pathway for cholesterol homeostasis. Science 1986;232:34–47.
82. Eden ER, Patel DD, Sun XM, Burden JJ, Themis M, Edwards M, et al. Restoration of LDL receptor function in cells from patients with autosomal recessive hypercholesterolemia by retroviral expression of ARH1. J Clin Invest 2002; 110:1695–702.
83. Norman D, Sun XM, Bourbon M, Knight BL, Naoumova RP, Soutar AK. Characterization of a novel cellular defect in patients with phenotypic homozygous familial hypercholesterolemia. J Clin Invest 1999;104:619–28.
84. Wilund KR, Yi M, Campagna F, Arca M, Zuliani G, Fellin R, et al. Molecular mechanisms of autosomal recessive hypercholesterolemia. Hum Mol Genet 2002;11:3019–30.
85. Sirinian MI, Belleudi F, Campagna F, Ceridono M, Garofalo T, Quagliarini F, et al. Adaptor protein ARH is recruited to the plasma membrane by low density lipoprotein (LDL) binding and modulates endocytosis of the LDL/LDL receptor complex in hepatocytes. J Biol Chem 2005;280: 38416–23.
86. Schafer DF, Sorrell MF. Hepatocellular carcinoma. Lancet 1999;353:1253–7.
87. Geller SA. Hepatitis B and hepatitis C. Clin Liver Dis 2002; 6:317–34.
88. Iino S. Natural history of hepatitis B and C virus infections. Oncology 2002;62:18–23.
89. Nakamoto Y, Guidotti LG, Kuhlen CV, Fowler P, Chisari FV. Immune pathogenesis of hepatocellular carcinoma. J Exp Med 1998;188:341–50.
90. Fujii C, Nakamoto Y, Lu P, Tsuneyama K, Popivanova BK, Kaneko S, et al. Aberrant expression of serine/threonine kinase Pim-3 in hepatocellular carcinoma development and its role in the proliferation of human hepatoma cell lines. Int J Cancer 2005;114:209–18.
91. Deneen B, Welford SM, Ho T, Hernandez F, Kurland I, Denny CT. PIM3 proto-oncogene kinase is a common transcriptional target of divergent EWS/ETS oncoproteins. Mol Cell Biol 2003;23:3897–908.
92. Dyson N. The regulation of E2F by pRB-family proteins. Genes Dev 1998;12:2245–62.
93. Phillips AC, Vousden KH. E2F-1 induced apoptosis. Apoptosis 2001;6:173–82.
94. Sola S, Ma X, Castro RE, Kren BT, Steer CJ, Rodrigues CM. Ursodeoxycholic acid modulates E2F-1 and p53 expression through a caspase-independent mechanism in transforming growth factor beta1-induced apoptosis of rat hepatocytes. J Biol Chem 2003;278:48831–8.
95. Fan G, Ma X, Kren BT, Steer CJ. Unbound E2F modulates TGF-beta1-induced apoptosis in HuH-7 cells. J Cell Sci 2002;115:3181–91.
96. Schwarz JK, Bassing CH, Kovesdi I, Datto MB, Blazing M, George S, et al. Expression of the E2F1 transcription factor overcomes type beta transforming growth factor-mediated growth suppression. Proc Natl Acad Sci U S A 1995;92: 483–7.
97. Botla R, Spivey JR, Aguilar H, Bronk SF, Gores GJ. Ursodeoxycholate (UDCA) inhibits the mitochondrial membrane permeability transition induced by glycochenodeoxycholate: a mechanism of UDCA cytoprotection. J Pharmacol Exp Ther 1995;272:930–8.
98. Rodrigues CM, Fan G, Ma X, Kren BT, Steer CJ. A novel role for ursodeoxycholic acid in inhibiting apoptosis by modulating mitochondrial membrane perturbation. J Clin Invest 1998;101:2790–9.
99. Rodrigues CM, Ma X, Linehan-Stieers C, Fan G, Kren BT, Steer CJ. Ursodeoxycholic acid prevents cytochrome c release in apoptosis by inhibiting mitochondrial membrane depolarization and channel formation. Cell Death Differ 1999;6:842–54.
100. Rodrigues CM, Sola S, Sharpe JC, Moura JJ, Steer CJ. Tauroursodeoxycholic acid prevents Bax-induced membrane perturbation and cytochrome C release in isolated mitochondria. Biochemistry 2003;42:3070–80.
101. Tanaka H, Makino Y, Miura T, Hirano F, Okamoto K, Komura K, et al. Ligand-independent activation of the glucocorticoid receptor by ursodeoxycholic acid. Repression of IFN-gamma-induced MHC class II gene expression via a glucocorticoid receptor-dependent pathway. J Immunol 1996;156:1601–8.
102. Miura T, Ouchida R, Yoshikawa N, Okamoto K, Makino Y, Nakamura T, et al. Functional modulation of the glucocorticoid receptor and suppression of NF-kappaB-dependent transcription by ursodeoxycholic acid. J Biol Chem 2001; 276:47371–8.
103. Bailly-Maitre B, de Sousa G, Boulukos K, Gugenheim J, Rahmani R. Dexamethasone inhibits spontaneous apoptosis in primary cultures of human and rat hepatocytes via Bcl-2 and Bcl-xL induction. Cell Death Differ 2001;8:279–88.
104. Yamamoto M, Fukuda K, Miura N, Suzuki R, Kido T, Komatsu Y. Inhibition by dexamethasone of transforming growth factor beta1-induced apoptosis in rat hepatoma cells:

a possible association with Bcl-xL induction. Hepatology 1998;27:959–66.

105. Almeida OF, Conde GL, Crochemore C, Demeneix BA, Fischer D, Hassan AH, et al. Subtle shifts in the ratio between pro- and antiapoptotic molecules after activation of corticosteroid receptors decide neuronal fate. FASEB J 2000;14:779–90.
106. Hassan AH, von Rosenstiel P, Patchev VK, Holsboer F, Almeida OF. Exacerbation of apoptosis in the dentate gyrus of the aged rat by dexamethasone and the protective role of corticosterone. Exp Neurol 1996;140:43–52.
107. Hassan AH, Patchev VK, von Rosenstiel P, Holsboer F, Almeida OF. Plasticity of hippocampal corticosteroid receptors during aging in the rat. FASEB J 1999;13:115–22.
108. McCullers DL, Herman JP. Mineralocorticoid receptors regulate bcl-2 and p53 mRNA expression in hippocampus. Neuroreport 1998;9:3085–9.
109. Nishi M, Ogawa H, Ito T, Matsuda KI, Kawata M. Dynamic changes in subcellular localization of mineralocorticoid receptor in living cells: in comparison with glucocorticoid receptor using dual-color labeling with green fluorescent protein spectral variants. Mol Endocrinol 2001; 15:1077–92.
110. Sola S, Castro RE, Kren BT, Steer CJ, Rodrigues CM. Modulation of nuclear steroid receptors by ursodeoxycholic acid inhibits TGF-beta1-induced E2F-1/p53-mediated apoptosis of rat hepatocytes. Biochemistry 2004;43:8429–38.
111. Schwabe RF, Uchinami H, Qian T, Bennett BL, Lemasters JJ, Brenner DA. Differential requirement for c-Jun NH2-terminal kinase in TNFalpha- and Fas-mediated apoptosis in hepatocytes. FASEB J 2004;18:720–2.
112. Bailly-Maitre B, de Sousa G, Zucchini N, Gugenheim J, Boulukos KE, Rahmani R. Spontaneous apoptosis in primary cultures of human and rat hepatocytes: molecular mechanisms and regulation by dexamethasone. Cell Death Differ 2002;9:945–55.
113. Krueger A, Schmitz I, Baumann S, Krammer PH, Kirchhoff S. Cellular FLICE-inhibitory protein splice variants inhibit different steps of caspase-8 activation at the CD95 death-inducing signaling complex. J Biol Chem 2001;276: 20633–40.
114. Conticello C, Pedini F, Zeuner A, Patti M, Zerilli M, Stassi G, et al. IL-4 protects tumor cells from anti-CD95 and chemotherapeutic agents via up-regulation of antiapoptotic proteins. J Immunol 2004;172:5467–77.
115. Leverkus M, Neumann M, Mengling T, Rauch CT, Brocker EB, Krammer PH, et al. Regulation of tumor necrosis factor-related apoptosis-inducing ligand sensitivity in primary and transformed human keratinocytes. Cancer Res 2000;60:553–9.
116. Okano H, Shiraki K, Inoue H, Kawakita T, Yamanaka T, Deguchi M, et al. Cellular FLICE/caspase-8-inhibitory protein as a principal regulator of cell death and survival in human hepatocellular carcinoma. Lab Invest 2003;83: 1033–43.
117. Oh HY, Namkoong S, Lee SJ, Por E, Kim CK, Billiar TR, et al. Dexamethasone protects primary cultured hepatocytes from death receptor-mediated apoptosis by upregulation of cFLIP. Cell Death Differ 2006;13:512–23.
118. Bhadriraju K, Hansen LK. Extracellular matrix-dependent myosin dynamics during G1-S phase cell cycle progression in hepatocytes. Exp Cell Res 2004;300:259–71.
119. Coutant A, Rescan C, Gilot D, Loyer P, Guguen-Guillouzo C, Baffet G. PI3K-FRAP/mTOR pathway is critical for hepatocyte proliferation whereas MEK/ERK supports both proliferation and survival. Hepatology 2002;36:1079–88.
120. Iijima Y, Laser M, Shiraishi H, Willey CD, Sundaravadivel B, Xu L, et al. c-Raf/MEK/ERK pathway controls protein kinase C-mediated p70S6K activation in adult cardiac muscle cells. J Biol Chem 2002;277:23065–75.
121. Bessard A, Coutant A, Rescan C, Ezan F, Fremin C, Courselaud B, et al. An MLCK-dependent window in late G1 controls S phase entry of proliferating rodent hepatocytes via ERK-p70S6K pathway. Hepatology 2006; 44:152–63.
122. Suzuki YJ, Forman HJ, Sevanian A. Oxidants as stimulators of signal transduction. Free Radic Biol Med 1997;22: 269–85.
123. Carmody RJ, Cotter TG. Signalling apoptosis: a radical approach. Redox Rep 2001;6:77–90.
124. Ueda S, Masutani H, Nakamura H, Tanaka T, Ueno M, Yodoi J. Redox control of cell death. Antioxid Redox Signal 2002;4:405–14.
125. Suzuki YJ. Growth factor signaling for cardioprotection against oxidative stress-induced apoptosis. Antioxid Redox Signal 2003;5:741–9.
126. Matsuzawa A, Ichijo H. Stress-responsive protein kinases in redox-regulated apoptosis signaling. Antioxid Redox Signal 2005;7:472–81.
127. Culmsee C, Mattson MP. p53 in neuronal apoptosis. Biochem Biophys Res Commun 2005;331:761–77.
128. Shiba D, Shimamoto N. Attenuation of endogenous oxidative stress-induced cell death by cytochrome P450 inhibitors in primary cultures of rat hepatocytes. Free Radic Biol Med 1999;27:1019–26.
129. Ishihara Y, Shiba D, Shimamoto N. Primary hepatocyte apoptosis is unlikely to relate to caspase-3 activity under sustained endogenous oxidative stress. Free Radic Res 2005; 39:163–73.
130. Li LY, Luo X, Wang X. Endonuclease G is an apoptotic DNase when released from mitochondria. Nature 2001;412: 95–9.
131. Van Loo G, Schotte P, van Gurp M, Demol H, Hoorelbeke B, Gevaert K, et al. Endonuclease G: a mitochondrial protein released in apoptosis and involved in caspase-independent DNA degradation. Cell Death Differ 2001;8: 1136–42.
132. Ishihara Y, Shimamoto N. Involvement of endonuclease G in nucleosomal DNA fragmentation under sustained endogenous oxidative stress. J Biol Chem 2006;281:6726–33.
133. Ding Y, Le XP, Zhang QX, Du P. Methylation and mutation analysis of p16 gene in gastric cancer. World J Gastroenterol 2003;9:423–6.
134. Okano M, Bell DW, Haber DA, Li E. DNA methyltransferases Dnmt3a and Dnmt3b are essential for de novo methylation and mammalian development. Cell 1999;99: 247–57.
135. Xu J, Fan H, Zhao ZJ, Zhang JQ, Xie W. Identification of potential genes regulated by DNA methyltransferase 3B in a hepatocellular carcinoma cell line by RNA interference and microarray analysis. Yi Chuan Xue Bao 2005;32:1115–27.
136. Yin M, Wheeler MD, Kono H, Bradford BU, Gallucci RM, Luster MI, et al. Essential role of tumor necrosis factor alpha in alcohol-induced liver injury in mice. Gastroenterology 1999;117:942–52.
137. Bradham CA, Plumpe J, Manns MP, Brenner DA, Trautwein C. Mechanisms of hepatic toxicity. I. TNF-induced liver injury. Am J Physiol 1998;275:G387–92.
138. Slomiany BL, Piotrowski J, Slomiany A. Chronic alcohol ingestion enhances tumor necrosis factor-alpha expression and salivary gland apoptosis. Alcohol Clin Exp Res 1997;21: 1530–3.

139. Lin HZ, Yang SQ, Zeldin G, Diehl AM. Chronic ethanol consumption induces the production of tumor necrosis factor-alpha and related cytokines in liver and adipose tissue. Alcohol Clin Exp Res 1998;22:231S–7S.
140. Deaciuc IV, D'Souza NB, Spitzer JJ. Tumor necrosis factor-alpha cell-surface receptors of liver parenchymal and non-parenchymal cells during acute and chronic alcohol administration to rats. Alcohol Clin Exp Res 1995;19:332–8.
141. Pastorino JG, Hoek JB. Ethanol potentiates tumor necrosis factor-alpha cytotoxicity in hepatoma cells and primary rat hepatocytes by promoting induction of the mitochondrial permeability transition. Hepatology 2000;31:1141–52.
142. Fernandez-Checa JC, Kaplowitz N, Garcia-Ruiz C, Colell A, Miranda M, Mari M, et al. GSH transport in mitochondria: defense against TNF-induced oxidative stress and alcohol-induced defect. Am J Physiol 1997;273:G7–17.
143. Hatano E, Brenner DA. Akt protects mouse hepatocytes from TNF-alpha- and Fas-mediated apoptosis through NK-kappa B activation. Am J Physiol Gastrointest Liver Physiol 2001;281:G1357–68.
144. Kennedy SG, Kandel ES, Cross TK, Hay N. Akt/Protein kinase B inhibits cell death by preventing the release of cytochrome c from mitochondria. Mol Cell Biol 1999;19: 5800–10.
145. Khwaja A. Akt is more than just a Bad kinase. Nature 1999; 401:33–4.
146. Pastorino JG, Shulga N, Hoek JB. TNF-alpha-induced cell death in ethanol-exposed cells depends on p38 MAPK signaling but is independent of Bid and caspase-8. Am J Physiol Gastrointest Liver Physiol 2003;285:G503–16.
147. Shulga N, Hoek JB, Pastorino JG. Elevated PTEN levels account for the increased sensitivity of ethanol-exposed cells to tumor necrosis factor-induced cytotoxicity. J Biol Chem 2005;280:9416–24.
148. Akira S, Hemmi H. Recognition of pathogen-associated molecular patterns by TLR family. Immunol Lett 2003;85: 85–95.
149. Alexopoulou L, Holt AC, Medzhitov R, Flavell RA. Recognition of double-stranded RNA and activation of NF-kappaB by Toll-like receptor 3. Nature 2001;413:732–8.
150. Hoebe K, Du X, Georgel P, Janssen E, Tabeta K, Kim SO, et al. Identification of Lps2 as a key transducer of MyD88-independent TIR signalling. Nature 2003;424:743–8.
151. Oshiumi H, Matsumoto M, Funami K, Akazawa T, Seya T. TICAM-1, an adaptor molecule that participates in Toll-like receptor 3-mediated interferon-beta induction. Nat Immunol 2003;4:161–7.
152. Yamamoto M, Sato S, Mori K, Hoshino K, Takeuchi O, Takeda K, et al. Cutting edge: a novel Toll/IL-1 receptor domain-containing adapter that preferentially activates the IFN-beta promoter in the Toll-like receptor signaling. J Immunol 2002;169:6668–72.
153. Yamamoto M, Sato S, Hemmi H, Hoshino K, Kaisho T, Sanjo H, et al. Role of adaptor TRIF in the MyD88-independent toll-like receptor signaling pathway. Science 2003;301:640–3.
154. Lund JM, Alexopoulou L, Sato A, Karow M, Adams NC, Gale NW, et al. Recognition of single-stranded RNA viruses by Toll-like receptor 7. Proc Natl Acad Sci U S A 2004;101: 5598–603.
155. Honda K, Sakaguchi S, Nakajima C, Watanabe A, Yanai H, Matsumoto M, et al. Selective contribution of IFN-alpha/beta signaling to the maturation of dendritic cells induced by double-stranded RNA or viral infection. Proc Natl Acad Sci U S A 2003;100:10872–7.
156. Edelmann KH, Richardson-Burns S, Alexopoulou L, Tyler KL, Flavell RA, Oldstone MB. Does Toll-like receptor 3 play a biological role in virus infections? Virology 2004;322: 231–8.
157. Yoneyama M, Kikuchi M, Natsukawa T, Shinobu N, Imaizumi T, Miyagishi M, et al. The RNA helicase RIG-I has an essential function in double-stranded RNA-induced innate antiviral responses. Nat Immunol 2004;5:730–7.
158. Li K, Chen Z, Kato N, Gale M Jr, Lemon SM. Distinct poly(I-C) and virus-activated signaling pathways leading to interferon-beta production in hepatocytes. J Biol Chem 2005;280:16739–47.
159. Noguchi M, Hirohashi S. Cell lines from non-neoplastic liver and hepatocellular carcinoma tissue from a single patient. In Vitro Cell Dev Biol Anim 1996;32:135–7.
160. Ikeda M, Sugiyama K, Mizutani T, Tanaka T, Tanaka K, Sekihara H, et al. Human hepatocyte clonal cell lines that support persistent replication of hepatitis C virus. Virus Res 1998;56:157–67.
161. Arima N, Kao CY, Licht T, Padmanabhan R, Sasaguri Y, Padmanabhan R. Modulation of cell growth by the hepatitis C virus nonstructural protein NS5A. J Biol Chem 2001;276: 12675–84.
162. Kato N. Molecular virology of hepatitis C virus. Acta Med Okayama 2001;55:133–59.
163. Ray RB, Ray R. Hepatitis C virus core protein: intriguing properties and functional relevance. FEMS Microbiol Lett 2001;202:149–56.
164. Reed KE, Rice CM. Overview of hepatitis C virus genome structure, polyprotein processing, and protein properties. Curr Top Microbiol Immunol 2000;242:55–84.
165. Dubourdeau M, Miyamura T, Matsuura Y, Alric L, Pipy B, Rousseau D. Infection of HepG2 cells with recombinant adenovirus encoding the HCV core protein induces p21(WAF1) down-regulation—effect of transforming growth factor beta. J Hepatol 2002;37:486–92.
166. Jung EY, Lee MN, Yang HY, Yu D, Jang KL. The repressive activity of hepatitis C virus core protein on the transcription of p21(waf1) is regulated by protein kinase A-mediated phosphorylation. Virus Res 2001;79:109–15.
167. Lu W, Lo SY, Chen M, Wu K, Fung YK, Ou JH. Activation of p53 tumor suppressor by hepatitis C virus core protein. Virology 1999;264:134–41.
168. Marusawa H, Hijikata M, Chiba T, Shimotohno K. Hepatitis C virus core protein inhibits Fas- and tumor necrosis factor alpha-mediated apoptosis via NF-kappaB activation. J Virol 1999;73:4713–20.
169. Ray RB, Steele R, Meyer K, Ray R. Hepatitis C virus core protein represses p21WAF1/Cip1/Sid1 promoter activity. Gene 1998;208:331–6.
170. Scholle F, Li K, Bodola F, Ikeda M, Luxon BA, Lemon SM. Virus-host cell interactions during hepatitis C virus RNA replication: impact of polyprotein expression on the cellular transcriptome and cell cycle association with viral RNA synthesis. J Virol 2004;78:1513–24.
171. Tsuchihara K, Hijikata M, Fukuda K, Kuroki T, Yamamoto N, Shimotohno K. Hepatitis C virus core protein regulates cell growth and signal transduction pathway transmitting growth stimuli. Virology 1999;258:100–7.
172. Dansako H, Naganuma A, Nakamura T, Ikeda F, Nozaki A, Kato N. Differential activation of interferon-inducible genes by hepatitis C virus core protein mediated by the interferon stimulated response element. Virus Res 2003;97:17–30.
173. Naganuma A, Nozaki A, Tanaka T, Sugiyama K, Takagi H, Mori M, et al. Activation of the interferon-inducible 2′-5′-oligoadenylate synthetase gene by hepatitis C virus core protein. J Virol 2000;74:8744–50.

174. Naganuma A, Dansako H, Nakamura T, Nozaki A, Kato N. Promotion of microsatellite instability by hepatitis C virus core protein in human non-neoplastic hepatocyte cells. Cancer Res 2004;64:1307–14.
175. Naka K, Dansako H, Kobayashi N, Ikeda M, Kato N. Hepatitis C virus NS5B delays cell cycle progression by inducing interferon-beta via Toll-like receptor 3 signaling pathway without replicating viral genomes. Virology 2006; 346:348–62.
176. MacDonald G, Shi L, Vande Velde C, Lieberman J, Greenberg AH. Mitochondria-dependent and -independent regulation of Granzyme B-induced apoptosis. J Exp Med 1999; 189:131–44.
177. Song E, Chen J, Su F, Wang M, Heemann U. Granzyme B inhibitor I reduces apoptotic cell death of allogeneic-transplanted hepatocytes in spleen. Transplant Proc 2001; 33:3274–5.
178. Wang J, Li W, Min J, Ou Q, Chen J. Fas siRNA reduces apoptotic cell death of allogeneic-transplanted hepatocytes in mouse spleen. Transplant Proc 2003;35:1594–5.
179. Kondo T, Suda T, Fukuyama H, Adachi M, Nagata S. Essential roles of the Fas ligand in the development of hepatitis. Nat Med 1997;3:409–13.
180. Kuhnel F, Zender L, Paul Y, Tietze MK, Trautwein C, Manns M, et al. NFkappaB mediates apoptosis through transcriptional activation of Fas (CD95) in adenoviral hepatitis. J Biol Chem 2000;275:6421–7.
181. Mundt B, Kuhnel F, Zender L, Paul Y, Tillmann H, Trautwein C, et al. Involvement of TRAIL and its receptors in viral hepatitis. FASEB J 2003;17:94–6.
182. Shi Y. Mechanisms of caspase activation and inhibition during apoptosis. Mol Cell 2002;9:459–70.
183. Nishimura Y, Hirabayashi Y, Matsuzaki Y, Musette P, Ishii A, Nakauchi H, et al. In vivo analysis of Fas antigen-mediated apoptosis: effects of agonistic anti-mouse Fas mAb on thymus, spleen and liver. Int Immunol 1997;9:307–16.
184. Zender L, Hutker S, Liedtke C, Tillmann HL, Zender S, Mundt B, et al. Caspase 8 small interfering RNA prevents acute liver failure in mice. Proc Natl Acad Sci U S A 2003; 100:7797–802.
185. Kanzler S, Galle PR. Apoptosis and the liver. Semin Cancer Biol 2000;10:173–84.
186. Eichhorst ST. Modulation of apoptosis as a target for liver disease. Expert Opin Ther Targets 2005;9:83–99.
187. Gressner AM, Weiskirchen R. The tightrope of therapeutic suppression of active transforming growth factor-beta: high enough to fall deeply? J Hepatol 2003;39:856–9.
188. Mizuguchi Y, Yokomuro S, Mishima T, Arima Y, Shimizu T, Kawahigashi Y, et al. Short hairpin RNA modulates transforming growth factor beta signaling in life-threatening liver failure in mice. Gastroenterology 2005;129:1654–62.
189. Rust C, Gores GJ. Apoptosis and liver disease. Am J Med 2000;108:567–74.
190. Siegel RM, Fleisher TA. The role of Fas and related death receptors in autoimmune and other disease states. J Allergy Clin Immunol 1999;103:729–38.
191. Canbay A, Higuchi H, Bronk SF, Taniai M, Sebo TJ, Gores GJ. Fas enhances fibrogenesis in the bile duct ligated mouse: a link between apoptosis and fibrosis. Gastroenterology 2002;123:1323–30.
192. Galle PR, Hofmann WJ, Walczak H, Schaller H, Otto G, Stremmel W, et al. Involvement of the CD95 (APO-1/Fas) receptor and ligand in liver damage. J Exp Med 1995;182: 1223–30.
193. Li XK, Fujino M, Sugioka A, Morita M, Okuyama T, Guo L, et al. Fulminant hepatitis by Fas-ligand expression in MRL-lpr/lpr mice grafted with Fas-positive livers and wild-type mice with Fas-mutant livers. Transplantation 2001;71: 503–8.
194. Song E, Lee SK, Wang J, Ince N, Ouyang N, Min J, et al. RNA interference targeting Fas protects mice from fulminant hepatitis. Nat Med 2003;9:347–51.
195. Bartenschlager R, Frese M, Pietschmann T. Novel insights into hepatitis C virus replication and persistence. Adv Virus Res 2004;63:71–180.
196. Randall G, Rice CM. Hepatitis C virus cell culture replication systems: their potential use for the development of antiviral therapies. Curr Opin Infect Dis 2001;14: 743–7.
197. Zeuzem S, Feinman SV, Rasenack J, Heathcote EJ, Lai MY, Gane E, et al. Peginterferon alfa-2a in patients with chronic hepatitis C. N Engl J Med 2000;343:1666–72.
198. Heathcote EJ, Shiffman ML, Cooksley WG, Dusheiko GM, Lee SS, Balart L, et al. Peginterferon alfa-2a in patients with chronic hepatitis C and cirrhosis. N Engl J Med 2000;343: 1673–80.
199. Kato N, Hijikata M, Ootsuyama Y, Nakagawa M, Ohkoshi S, Sugimura T, et al. Molecular cloning of the human hepatitis C virus genome from Japanese patients with non-A, non-B hepatitis. Proc Natl Acad Sci U S A 1990;87:9524–8.
200. Bartenschlager R, Lohmann V. Replication of hepatitis C virus. J Gen Virol 2000;81:1631–48.
201. Thomas DL. Hepatitis C epidemiology. Curr Top Microbiol Immunol 2000;242:25–41.
202. McHutchison JG, Patel K. Future therapy of hepatitis C. Hepatology 2002;36:S245–52.
203. Kim WR. The burden of hepatitis C in the United States. Hepatology 2002;36:S30–4.
204. McHutchison JG. Hepatitis C advances in antiviral therapy: what is accepted treatment now? J Gastroenterol Hepatol 2002;17:431–41.
205. McCaffrey AP, Meuse L, Pham TT, Conklin DS, Hannon GJ, Kay MA. RNA interference in adult mice. Nature 2002; 418:38–9.
206. Wilson JA, Jayasena S, Khvorova A, Sabatinos S, Rodrigue-Gervais IG, Arya S, et al. RNA interference blocks gene expression and RNA synthesis from hepatitis C replicons propagated in human liver cells. Proc Natl Acad Sci U S A 2003;100:2783–8.
207. Wilson JA, Richardson CD. Hepatitis C virus replicons escape RNA interference induced by a short interfering RNA directed against the NS5b coding region. J Virol 2005; 79:7050–8.
208. Kapadia SB, Brideau-Andersen A, Chisari FV. Interference of hepatitis C virus RNA replication by short interfering RNAs. Proc Natl Acad Sci U S A 2003;100:2014–8.
209. Randall G, Grakoui A, Rice CM. Clearance of replicating hepatitis C virus replicon RNAs in cell culture by small interfering RNAs. Proc Natl Acad Sci U S A 2003;100:235–40.
210. Blight KJ, McKeating JA, Rice CM. Highly permissive cell lines for subgenomic and genomic hepatitis C virus RNA replication. J Virol 2002;76:13001–14.
211. Choo QL, Richman KH, Han JH, Berger K, Lee C, Dong C, et al. Genetic organization and diversity of the hepatitis C virus. Proc Natl Acad Sci U S A 1991;88:2451–5.
212. Okamoto H, Okada S, Sugiyama Y, Kurai K, Iizuka H, Machida A, et al. Nucleotide sequence of the genomic RNA of hepatitis C virus isolated from a human carrier: comparison with reported isolates for conserved and divergent regions. J Gen Virol 1991;72:2697–704.
213. Yokota T, Sakamoto N, Enomoto N, Tanabe Y, Miyagishi M, Maekawa S, et al. Inhibition of intracellular hepatitis C

virus replication by synthetic and vector-derived small interfering RNAs. EMBO Rep 2003;4:602–8.
214. Kronke J, Kittler R, Buchholz F, Windisch MP, Pietschmann T, Bartenschlager R, et al. Alternative approaches for efficient inhibition of hepatitis C virus RNA replication by small interfering RNAs. J Virol 2004;78:3436–46.
215. Takigawa Y, Nagano-Fujii M, Deng L, Hidajat R, Tanaka M, Mizuta H, et al. Suppression of hepatitis C virus replicon by RNA interference directed against the NS3 and NS5B regions of the viral genome. Microbiol Immunol 2004;48: 591–8.
216. Kruger M, Beger C, Welch PJ, Barber JR, Manns MP, Wong-Staal F. Involvement of proteasome alpha-subunit PSMA7 in hepatitis C virus internal ribosome entry site-mediated translation. Mol Cell Biol 2001;21:8357–64.
217. Ma WJ, Cheng S, Campbell C, Wright A, Furneaux H. Cloning and characterization of HuR, a ubiquitously expressed Elav-like protein. J Biol Chem 1996;271:8144–51.
218. Spangberg K, Wiklund L, Schwartz S. HuR, a protein implicated in oncogene and growth factor mRNA decay, binds to the 3′ ends of hepatitis C virus RNA of both polarities. Virology 2000;274:378–90.
219. Korf M, Jarczak D, Beger C, Manns MP, Kruger M. Inhibition of hepatitis C virus translation and subgenomic replication by siRNAs directed against highly conserved HCV sequence and cellular HCV cofactors. J Hepatol 2005; 43:225–34.
220. Gomez-Gonzalo M, Carretero M, Rullas J, Lara-Pezzi E, Aramburu J, Berkhout B, et al. The hepatitis B virus X protein induces HIV-1 replication and transcription in synergy with T-cell activation signals: functional roles of NF-kappaB/NF-AT and SP1-binding sites in the HIV-1 long terminal repeat promoter. J Biol Chem 2001;276: 35435–43.
221. Gong G, Waris G, Tanveer R, Siddiqui A. Human hepatitis C virus NS5A protein alters intracellular calcium levels, induces oxidative stress, and activates STAT-3 and NF-kappa B. Proc Natl Acad Sci U S A 2001;98:9599–604.
222. Matskevich AA, Strayer DS. Exploiting hepatitis C virus activation of NFkappaB to deliver HCV-responsive expression of interferons alpha and gamma. Gene Ther 2003;10: 1861–73.
223. Strayer DS, Feitelson M, Sun B, Matskevich AA. Paradigms for conditional expression of RNA interference molecules for use against viral targets. Methods Enzymol 2005;392: 227–41.
224. Hamazaki H, Ujino S, Miyano-Kurosaki N, Shimotohno K, Takaku H. Inhibition of hepatitis C virus RNA replication by short hairpin RNA synthesized by T7 RNA polymerase in hepatitis C virus subgenomic replicons. Biochem Biophys Res Commun 2006;343:988–94.
225. Seeger C, Mason WS. Hepatitis B virus biology. Microbiol Mol Biol Rev 2000;64:51–68.
226. Beasley RP, Hwang LY, Lin CC, Chien CS. Hepatocellular carcinoma and hepatitis B virus. A prospective study of 22 707 men in Taiwan. Lancet 1981;2:1129–33.
227. Dienstag JL, Perrillo RP, Schiff ER, Bartholomew M, Vicary C, Rubin M. A preliminary trial of lamivudine for chronic hepatitis B infection. N Engl J Med 1995;333:1657–61.
228. Hadziyannis SJ, Tassopoulos NC, Heathcote EJ, Chang TT, Kitis G, Rizzetto M, et al. Long-term therapy with adefovir dipivoxil for HBeAg-negative chronic hepatitis B. N Engl J Med 2005;352:2673–81.
229. Liaw YF, Sung JJ, Chow WC, Farrell G, Lee CZ, Yuen H, et al. Lamivudine for patients with chronic hepatitis B and advanced liver disease. N Engl J Med 2004;351:1521–31.
230. Marcellin P, Lau GK, Bonino F, Farci P, Hadziyannis S, Jin R, et al. Peginterferon alfa-2a alone, lamivudine alone, and the two in combination in patients with HBeAg-negative chronic hepatitis B. N Engl J Med 2004;351:1206–17.
231. Manesis EK, Hadziyannis SJ. Interferon alpha treatment and retreatment of hepatitis B e antigen-negative chronic hepatitis B. Gastroenterology 2001;121:101–9.
232. McCaffrey AP, Nakai H, Pandey K, Huang Z, Salazar FH, Xu H, et al. Inhibition of hepatitis B virus in mice by RNA interference. Nat Biotechnol 2003;21:639–44.
233. Giladi H, Ketzinel-Gilad M, Rivkin L, Felig Y, Nussbaum O, Galun E. Small interfering RNA inhibits hepatitis B virus replication in mice. Mol Ther 2003;8:769–76.
234. Konishi M, Wu CH, Wu GY. Inhibition of HBV replication by siRNA in a stable HBV-producing cell line. Hepatology 2003;38:842–50.
235. Shlomai A, Shaul Y. Inhibition of hepatitis B virus expression and replication by RNA interference. Hepatology 2003; 37:764–70.
236. Hamasaki K, Nakao K, Matsumoto K, Ichikawa T, Ishikawa H, Eguchi K. Short interfering RNA-directed inhibition of hepatitis B virus replication. FEBS Lett 2003;543:51–4.
237. Ying C, De Clercq E, Neyts J. Selective inhibition of hepatitis B virus replication by RNA interference. Biochem Biophys Res Commun 2003;309:482–4.
238. Klein C, Bock CT, Wedemeyer H, Wustefeld T, Locarnini S, Dienes HP, et al. Inhibition of hepatitis B virus replication in vivo by nucleoside analogues and siRNA. Gastroenterology 2003;125:9–18.
239. Chen Y, Du D, Wu J, Chan CP, Tan Y, Kung HF, et al. Inhibition of hepatitis B virus replication by stably expressed shRNA. Biochem Biophys Res Commun 2003;311:398–404.
240. Wu Y, Huang AL, Tang N, Zhang BQ, Lu NF. Specific antiviral effects of RNA interference on replication and expression of hepatitis B virus in mice. Chin Med J (Engl) 2005; 118:1351–6.
241. Morrissey DV, Blanchard K, Shaw L, Jensen K, Lockridge JA, Dickinson B, et al. Activity of stabilized short interfering RNA in a mouse model of hepatitis B virus replication. Hepatology 2005;41:1349–56.
242. Morrissey DV, Lockridge JA, Shaw L, Blanchard K, Jensen K, Breen W, et al. Potent and persistent in vivo anti-HBV activity of chemically modified siRNAs. Nat Biotechnol 2005;23:1002–7.
243. Uprichard SL, Boyd B, Althage A, Chisari FV. Clearance of hepatitis B virus from the liver of transgenic mice by short hairpin RNAs. Proc Natl Acad Sci U S A 2005;102:773–8.
244. Wu HL, Huang LR, Huang CC, Lai HL, Liu CJ, Huang YT, et al. RNA interference-mediated control of hepatitis B virus and emergence of resistant mutant. Gastroenterology 2005;128:708–16.
245. Carmona S, Ely A, Crowther C, Moolla N, Salazar FH, Marion PL, et al. Effective inhibition of HBV replication in vivo by anti-HBx short hairpin RNAs. Mol Ther 2006;13: 411–21.
246. Kim YH, Lee JH, Paik NW, Rho HM. RNAi-based knockdown of HBx mRNA in HBx-transformed and HBV-producing human liver cells. DNA Cell Biol 2006; 25:412–7.
247. Chen CC, Ko TM, Ma HI, Wu HL, Xiao X, Li J, et al. Long-term inhibition of hepatitis B virus in transgenic mice by double-stranded adeno-associated virus 8-delivered short hairpin RNA. Gene Ther 2007;14:11–9.

J Pharmacol Sci **103**, 159 – 167 (2007)

Journal of Pharmacological Sciences

©2007 The Japanese Pharmacological Society

Full Paper

Caspase Cascade Proceeds Rapidly After Cytochrome *c* Release From Mitochondria in Tumor Necrosis Factor-α-Induced Cell Death

Hiroshi Kawai[1,3,*], Takuo Suzuki[1], Tetsu Kobayashi[1], Akiko Ishii-Watabe[1], Haruna Sakurai[2], Hisayuki Ohata[2], Kazuo Honda[2], Kazutaka Momose[2], Takao Hayakawa[1], and Toru Kawanishi[1,#]

[1]*Division of Biological Chemistry and Biologicals, National Institute of Health Sciences, Tokyo 158-8501, Japan*
[2]*Department of Pharmacology, School of Pharmaceutical Sciences, Showa University, Tokyo 142-8555, Japan*
[3]*Faculty of Pharmaceutical Sciences, Josai International University, Chiba 283-8555, Japan*

Received August 2, 2006; Accepted December 2, 2006

Abstract. The caspase activation cascade and mitochondrial changes are major biochemical reactions in the apoptotic cell death machinery. We attempted to clarify the temporal relationship between caspase activation, cytochrome *c* release, mitochondrial depolarization, and morphological changes that take place during tumor necrosis factor (TNF)-α-induced cell death in HeLa cells. These reactions were analyzed at the single-cell level with 0.5 – 1 min resolution by using green fluorescent protein (GFP)-variant-derived probes and chemical probes. Cytochrome *c* release, caspase activation, and cellular shrinkage were always observed in this order within 10 min in all dying cells. This sequence of events was thus considered a critical pathway of cell death. Mitochondrial depolarization was also observed in all dying cells observed, but frequently occurred after caspase activation and cellular shrinkage. Mitochondrial depolarization is therefore likely to be a reaction that does not induce caspase activation and subsequent cellular shrinkage. Mitochondrial changes are important for apoptotic cell death; moreover, cytochrome *c* release, and not depolarization, is a key reaction related to cell death. In addition, we also found that the apoptotic pathway proceeds only when cells are exposed to TNF-α. These findings suggest that the entire cell death process proceeds rapidly during TNF-α exposure.

Keywords: tumor necrosis factor (TNF)-α, cytochrome *c*, mitochondrial depolarization, caspase, real-time imaging

Introduction

Apoptosis is a mechanism of cell death that is mediated by various intracellular reactions. A family of cysteine proteases, the caspases, forms the activation cascade, and these proteases play a central role in the apoptotic cell death machinery (1, 2). The caspases usually exist as pro-proteins in living cells and are activated by cleavage at the time when cell death is induced. In an early phase of the cell death process, initiator caspases are activated, which in turn activate effector caspases (3 – 7). Activated effector caspases cleave a number of different target proteins, and this cleavage leads ultimately to apoptotic cell death (8, 9). Mitochondria also play an important role in the cell death process (10 – 13). Cellular stresses induce mitochondrial changes, including an increase in outer mitochondrial membrane permeability; various mitochondrial proteins such as cytochrome *c* (cyt.*c*) and second mitochondrial activator of caspases (Smac) are released into the cytosol. Released proteins directly or indirectly regulate caspase activation and/or other reactions, which eventually induce cell death.

Various factors in the cell death process have been identified, but correlation among these factors remains unclear. Cell death events such as caspase activation and mitochondrial changes are rapid processes, and the onset of these events varies between individual cells (14 – 17). So, it is difficult to determine how and when such

*Corresponding author (affiliation #3). hkawai@jiu.ac.jp
#Present affiliation: Division of Drugs, National Institute of Health Sciences, Tokyo 158-8501, Japan
Published online in J-STAGE: February 8, 2007
doi: 10.1254/jphs.FP0060877

reactions occur in cells as based on analyses of cell populations, which can only be used to detect an average value for a large number of individual cells. In order to gain a better understanding of the cell death mechanism, simultaneous multi-events analyses should be conducted at the single-cell level and with high spatial and temporal resolution. Real-time imaging with confocal microscopy is a powerful method of detecting the manner in which such rapid intracellular reactions take place (18, 19).

Fluorescence resonance energy transfer (FRET) is useful for imaging analyses. Variants of green fluorescent protein (GFP) are currently widely employed; several families of fluorescent proteins have recently been reported to be useful for FRET analysis (19 – 22). Previously, we developed genetically-encoded sensors for caspase activation that consist of two fluorescent proteins linked by a small peptide (23, 24). Cyan-, green-, yellow-, and red-fluorescent proteins (CFP, GFP, YFP, DsRed) were used in combination as the fluorescent proteins. The small peptide was derived from a substrate of caspase, poly(ADP-ribose)polymerase; this fusion protein was primarily cleaved by caspase 3 (23). The sensor protein exhibits FRET in its intact form. However, in the presence of active caspase, the peptide is cleaved, and the two fluorescent proteins are rendered far apart; in this case, the sensor protein no longer exhibits any FRET. Caspase activation is detected as a reduction in FRET. We have previously reported that the use of various color combinations facilitates real-time imaging analysis. In particular, GFP-DsRed and YFP-DsRed have been shown to be as sensitive as CFP-YFP, which is commonly used as the FRET pair. FRET probes that consist of such color variations may be useful for simultaneous multi-event imaging (24).

In this study, we used the YFP-DsRed version of the effector-caspase sensor (YRec), CFP-tagged cyt.*c* (cyt.*c*-CFP), and tetramethylrhodamine methyl ester (TMRM) in order to detect caspase activation, cyt.*c* release from the mitochondria, and mitochondrial depolarization, respectively. By applying two of these probes simultaneously, two events could be monitored in the same cell, and the temporal relationships between caspase activation and mitochondrial changes could be examined at the single-cell level. In addition, we also analyzed the interval from tumor necrosis factor (TNF)-α exposure to cellular shrinkage by analyzing the cell population in order to investigate time course of the whole cell death process.

Materials and Methods

Plasmid construction

A plasmid encoding YRec, YFP-peptide-DsRed, was generated as previously reported (24). The sequence encoding the 11 amino acids at the C-terminus of YFP was eliminated in this construct. The C-terminal-truncated forms of the YFP gene were generated by PCR with primers containing the NheI site or the BspEI site and pEYFP-C1 (Clontech, Palo Alto, CA, USA) as a template, and the restricted fragment was inserted into the NheI/BspEI sites of pEYFP-C1 in order to generate a plasmid carrying truncated YFP. The oligonucleotides encoding the caspase's substrate sequence was inserted into the BspEI – AgeI site of the p(truncated YFP)-C1 vector to generate pYFP-PARP. The substrate sequence was derived from PARP (KRKGDEVDGVDE, 5'-CCGGAAAGAGAAAAGG CGATGAGGTGGATGGAGTGGATGAA-3' and 5'-CCGGTTCATCCACTCCATCCACCTCATCGCCTTT TCTCTTT-3'). DsRed was generated from pDsRed2-C1(Clontech) by PCR, at the AgeI/NotI sites, and the restricted fragment was inserted into the AgeI – NotI sites of pYFP-PARP to generate a plasmid carrying YFP-PARP-DsRed2 (YRec). YRec was cleaved by caspase-3 (23, 24).

Cyt.*c* was cloned from HeLa cells by RT-PCR with a primer pair (5'-TCGCTAGCGCTCCGGAGAATTAAA TATGGGTATG-3' and 5'-CGAGGATCCCTCATTAG TAGCTTTTTTGAG-3'), and the restricted fragment was inserted into the NheI – BamHI sites of the pECFP-N1 vector to generate a plasmid carrying cyt.*c*-CFP. All cloned sequences were verified by sequencing.

Cell culture and transfection

HeLa cells were cultured in DMEM (Sigma-Aldrich, St. Louis, MO, USA) supplemented with 100 units/ml of penicillin G, 100 μg/ml of streptomycin, and 10% fetal calf serum (GIBCO). The plasmid encoding the fluorescent probes was transfected into HeLa cells using Effectene Transfection Reagent (QIAGEN, Hilden, Germany) according to the manufacturer's instructions. After being incubated for 12 – 24 h with the transfection reagent, the cells were washed with PBS and cultivated on dishes suitable for an assay in medium containing 500 μg/ml of G418 for an additional 1 – 3 days until the assay was performed. We found that the cultivation period had no effect on cell death events after TNF-α treatment.

Bioimaging with fluorescence microscopy

Transfected cells were cultured on a cover glass (25-mm diameter, 0.15 – 0.18-mm thickness) for 1 – 3 days. Cells were treated with TNF-α (100 ng/ml, dissolved in PBS) and cycloheximide (10 μg/ml, dissolved in DMSO) and then were incubated under the usual culture conditions for 1 – 2 h prior to the analysis.

Table 1. Measurement conditions for real-time analysis by LSM510

Probe	Excitation (nm)	Beam splitter (nm)	Emission (nm)
Cyt.*c*-CFP	458	515	467.5 – 497.5
YRec	488	545	505 – 530 (donor)[a]
			560 – 615 (acceptor)[a]
TMRM	543	545	560 –[b]

[a]Emitted fluorescence was separated by a 545 dichroic mirror, and the fluorescence of the donor (YFP) and that of the acceptor (DsRed) was obtained via a band-pass emission filter. [b]A long-pass filter (LP560) was used.

Tetramethylrhodamine methyl ester (TMRM; 50 nM, dissolved in DMSO) was added to each sample 20 – 30 min prior to the analysis, when the mitochondrial membrane potential was to be measured (23, 25). Analyses were carried out by confocal laser scanning fluorescent microscopy using a Carl Zeiss LSM510 system (Carl Zeiss, Jena, Germany). During the observations, the media were buffered with 10 mM HEPES buffer (pH 7.4), and the cells were maintained at 35°C – 37°C. DIC images and grayscale images for fluorescence channels were obtained in 0.5- or 1-min intervals. Excitation lights for the cyt.*c*-CFP (458 nm) and YRec (488 nm) were provided by an Ar laser with a 458 or a 488 dichroic mirror, respectively. Excitation lights for the TMRM (543 nm) were provided by a HeNe laser with a 543 dichroic mirror. Images of the probes were obtained separately using a dichroic mirror and band-pass or long-pass emission filters, as indicated in Table 1. Contamination of the fluorescence between channels was negligible under these conditions (data not shown). For analyses involving YRec or TMRM, images were processed and quantified using MetaFluor software as follows: The average pixel intensity of the fluorescence of the entire cell region was determined for each channel. In the case of YRec, the ratio value was calculated as the average pixel value of the fluorescence ratio, (fluorescent intensity for the acceptor channel) /(fluorescent intensity for the donor channel), in the entire cell region. As the cells changed morphologically during the observation, the entire cell region was assessed separately for each image.

Simultaneous measurement of two probes was performed according to the multi-track scanning mode, in which two sets of excitation-detection conditions were used in alternation. For cyt.*c*-CFP and YRec, CFP fluorescence induced by excitation at 458 nm was measured in the first track, and YFP and DsRed fluorescence induced by excitation at 488 nm was measured in the second track. For cyt.*c*-CFP and TMRM, CFP fluorescence induced by excitation at 458 nm was measured in the first track, and TMRM fluorescence induced by excitation at 543 nm was measured in the second track. The scanning time difference between tracks was ca. 3 – 8 s, which was not significant in the temporal analysis.

Analysis of cell survival rate

HeLa cells were cultured in 96-well plastic plates to 80% – 90% confluency and were then treated with TNF-*α*. After the indicated culture durations, the cells were treated with Alamar Blue (Dainippon Pharmaceutical, Osaka) according to the manufacturer's instructions. Cell survival was measured as fluorescence at 590 nm induced by excitation at 540 nm. Fluorescence was measured using FlexStation (Molecular Devices, Sunnyvale, CA, USA).

Results

Simultaneous imaging of cyt.c-CFP and caspase sensor

HeLa cells expressing both cyt.*c*-CFP and YRec were treated with TNF-*α*, and changes in fluorescence were observed. Figure 1A shows DIC images, fluorescent images of CFP, and fluorescence ratio (DsRed/YFP) images of YRec during cell death. Images were obtained every 30 s; therefore, we were able to identify the time points of these events at a resolution period of 30 s. The CFP fluorescence indicated cyt.*c*-CFP localization, and the fluorescence ratio (DsRed/YFP) indicated caspase activation. CFP fluorescence was localized in the mitochondria at 280.5 min, and it was delocalized at 281.0 min, indicating that cyt.*c*-CFP was released during this period. The images shown in Fig. 1A indicate that this cell started to shrink at 286.5 – 287.0 min.

When the caspase was activated in a cell, the YRec was cleaved, which led to a reduction in the FRET from YFP to DsRed. Thus, a reduction in the fluorescence ratio (DsRed/YFP) reflected caspase activation. As shown in Fig. 1B, the fluorescence ratio decreased dramatically at 283.5 min in the cell shown here, thus indicating the initiation of caspase activation at this point in time. The increase in DsRed fluorescence

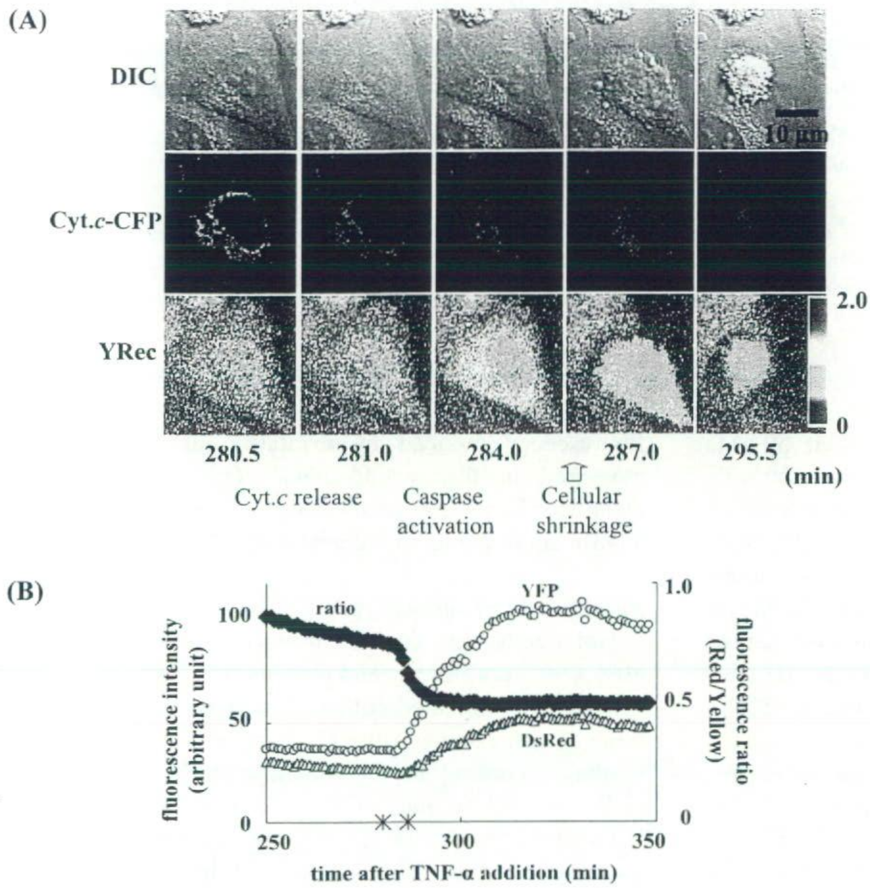

Fig. 1. Cyt.*c*-CFP release and caspase activation were monitored simultaneously in the same cells. A: DIC (upper), images showing the fluorescence of CFP (middle) and the fluorescence ratio of DsRed and YFP (DsRed /YFP, lower) during cell death are shown in pseudocolor. CFP and DsRed/YFP indicate the localization of cyt.*c*-CFP and caspase activation, respectively. B: Changes in YRec fluorescence in the cell shown in panel A were plotted. YFP and DsRed are shown with their fluorescence ratios. The asterisks indicate time points at which cyt.*c*-CFP were released and cell shrinkage was observed. The horizontal axis represents the point in time after the addition of TNF-α.

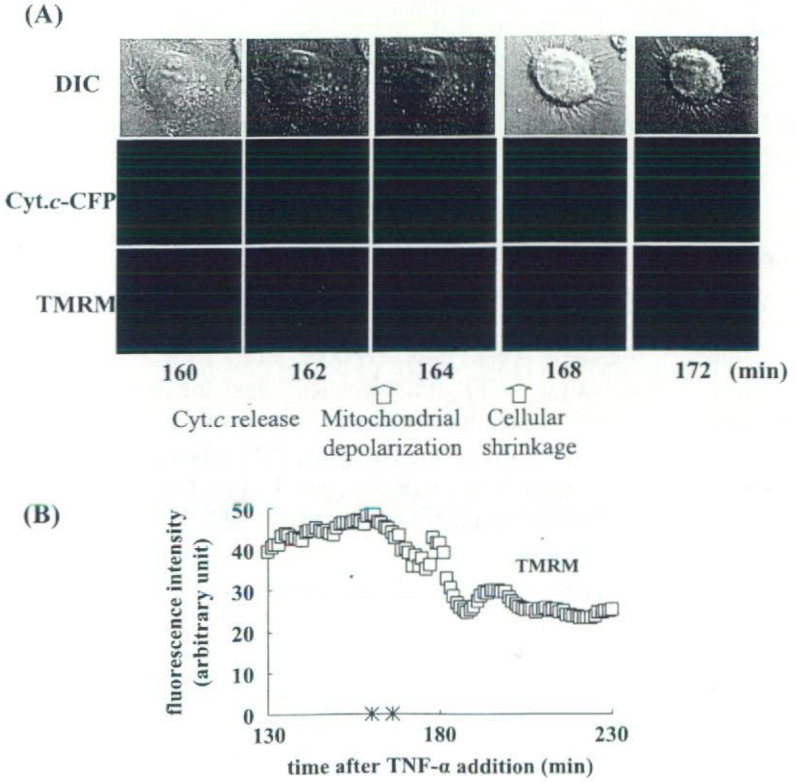

Fig. 2. Cyt.*c*-CFP release and mitochondrial depolarization were monitored simultaneously in the same cell. A: DIC (upper), images showing the fluorescence of CFP (middle) and the fluorescence of TMRM (lower) during cell death are shown in pseudocolor. CFP and TMRM fluorescence indicate the localization of cyt.*c*-CFP and the mitochondrial membrane potential, respectively. B: Changes in TMRM fluorescence of the cells in panel A during cell death were plotted. The asterisks indicate time points at which cyt.*c*-CFP were released and cell shrinkage was observed. The horizontal axis represents the point in time after the addition of TNF-α.

observed after this time point was unexpected, but is thought to have been the result of cellular shrinkage. Because the cell volume was reduced, the DsRed became concentrated, and the fluorescence increased. The reduction in the fluorescence ratio clearly indicated a reduction in FRET, which indicated both the cleavage of YRec as well as caspase activation. The asterisks indicate the time point of cyt.*c*-CFP release and cellular shrinkage, as determined based on the results shown in Fig. 1A. In this cell, cyt.*c*-CFP was released 280.5 min after the addition of TNF-α, and caspase activation was initiated 3 min after cyt.*c*-CFP release; the cell then started to shrink 3 min after caspase activation. Cyt.*c*-CFP release, caspase activation, and cellular shrinkage were observed in this order in all of the dying cells examined.

Simultaneous imaging of cyt.c-CFP and TMRM

HeLa cells expressing cyt.*c*-CFP were treated with TMRM and TNF-α. Delocalization of cyt.*c*-CFP and mitochondrial depolarization were observed with a resolution period of 1 min. All dying cells exhibited cyt.*c*-CFP release, mitochondrial depolarization, and shrinkage of the cell body. Figure 2A shows a typical fluorescent image of a dying cell. In this cell, cyt.*c*-CFP was released at 161 min, and cell shrinkage began at 167 min after the addition of TNF-α. Changes in TMRM fluorescence are plotted in Fig. 2B. TMRM fluorescence started to decrease at 164 min, thus indicating that the mitochondria started to depolarize at this point in time.

In a comparison of the starting points of these three events, it was found that the release of cyt.*c*-CFP always preceded mitochondrial depolarization and cellular shrinkage. Mitochondrial depolarization was observed earlier than cellular shrinkage in this particular cell, but was observed later in other cells. The temporal order of the timing of the initiation of mitochondrial depolarization and cellular shrinkage was not consistent. Mitochondrial depolarization preceded cellular shrinkage in 4 of the 10 cells, and cellular shrinkage preceded mitochondrial depolarization in 6 of the cells observed here.

Temporal relationships between mitochondrial changes, caspase activation, and cellular shrinkage

We observed 10 – 22 cells in each of these experiments, the results of which are shown in Figs. 1 and 2. We then determined the timing of cyt.*c* release, cellular shrinkage, and mitochondrial depolarization, or caspase activation in each cell. To clarify the temporal relationships between these cellular events, relative timing was

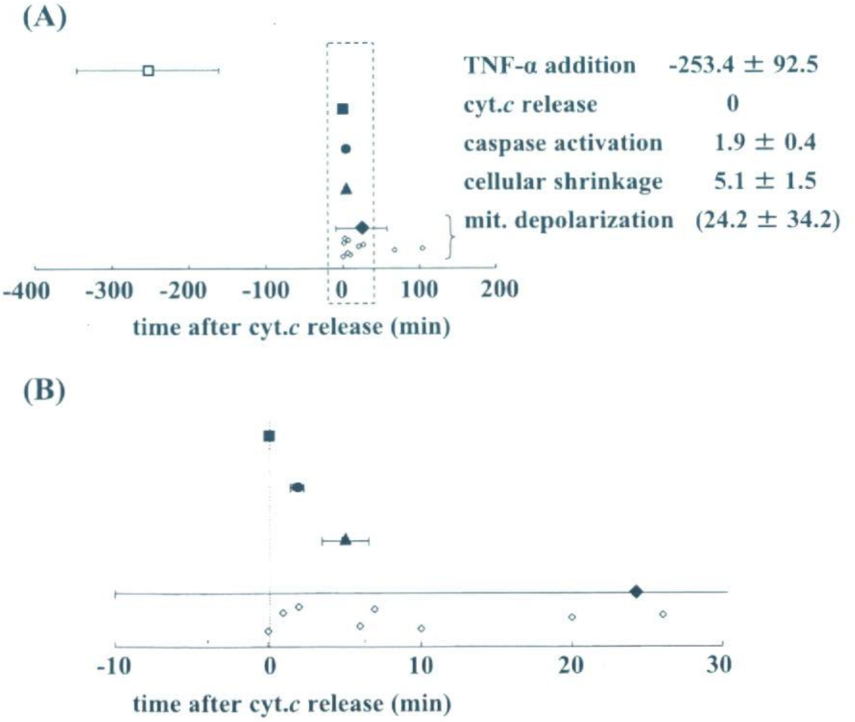

Fig. 3. Temporal relationship between mitochondrial changes and caspase activation. A: Relative timing of TNF-α addition (open square), cyt.*c* release (closed square), caspase activation (closed circle), cellular shrinkage (closed triangle), and mitochondrial depolarization (closed and open diamond) is shown with respect to time after cyt.*c* release. B: Shows a magnification of panel A.

determined as follows: the time point of cyt.*c* release was considered as time 0 in each of the individual cells. We calculated the relative timing of each of the observed events for each cell, and the results are plotted in Fig. 3. TNF-α treatment, cyt.*c* release, caspase activation, and cellular shrinkage are indicated as the mean ± S.D. Since mitochondrial depolarization did not give a normal distribution, all data for mitochondrial depolarization were plotted. Each plot represents the results from a single cell. Figure 3B shows magnification at around time 0.

The relative timing of TNF-α treatment and mitochondrial depolarization was found to deviate substantially, whereas the relative timing of caspase activation and cellular shrinkage gave only a small deviation. A substantial amount of time was required for the initiation of cyt.*c* release, and the duration varied between cells; however, after cyt.*c* release, the subsequent reactions occurred rapidly. After cyt.*c* release, cells are unable to stop or delay the cell death process.

Mitochondrial depolarization occurred before both caspase activation and cellular shrinkage in some of the cells (n = 4), but mitochondrial depolarization occurred after caspase activation and cellular shrinkage in other cells (n = 6). This finding suggests that mitochondrial depolarization is not necessary for either caspase activation or cellular shrinkage. Mitochondrial depolarization has been consistently reported as being associated with cell death, but it is not thought to be a critical step in the induction of apoptotic cell death.

Effects of the duration of TNF-α treatment

At the first step of TNF-α-induced cell death, TNF-α binds with its receptor on the cell surface, and an extracellular signal is transferred into the cell. After this step, Bid transfers the signal to the mitochondria, and then cyt.*c* is released from the mitochondria to the cytosol. Our results shown in Fig. 3 indicate that these processes took about 4 h. In order to analyze the timing of the onset of the earliest steps, we attempted to determine the point in time at which the first step started. To this end, we changed the duration of TNF-α exposure and measured the resulting cell survival rate. Cells were divided to two groups, as shown in Fig. 4A, and the cells were exposed to TNF-α for 0 – 12 h. In group A, the survival rate was measured immediately after TNF-α exposure. In group B, TNF-α was washed off after the indicated exposure time, and the cells were cultured in fresh medium without TNF-α for an additional 6 – 11 h, and the survival rate was then measured. If the cell death process proceeded after the removal of TNF-α, the survival rate would be expected to be reduced due to the additional culture period after the removal of TNF-α. In other words, more cells would be expected to have died in group B than in group A with the same amount of TNF-α exposure time.

The results showed that the survival rate decreased with increasing TNF-α exposure time (Fig. 4B). However, the survival rate did not decrease after TNF-α removal. This result suggests that the dead cells in group B had died during the period of TNF-α exposure, and that those cells that had survived during TNF-α exposure did not die after the removal of TNF-α. Thus, the cell death process is likely to proceed only when the cells were exposed to TNF-α. The survival rate in group B increased when cells were exposed TNF-α for 6 h. The biological meaning of this increase was unknown; however, this result did not disturb our conclusion.

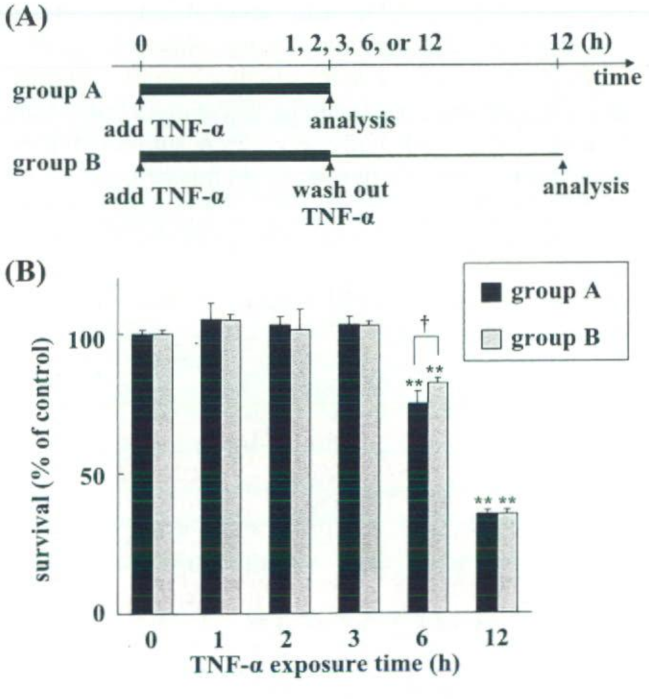

Fig. 4. Cell survival rate after TNF-α exposure. Panel A: Experimental design of the TNF-α exposure analysis. Thick lines represent the incubation in the presence of TNF-α, and thin line represents the incubation in the absence of TNF-α. In group A, cells were exposed to TNF-α for the indicated amount of time, and the cell survival rate was measured immediately. In group B, cells were exposed in the same manner as that used for group A. Then, the TNF-α was washed out, and the cells were cultured in fresh media for 6 – 11 h. Then, the cell survival rate was measured. The total duration of the culture period after the onset of TNF-α exposure was 12 h in group B. Panel B: The cells in groups A and B were exposed to TNF-α for 1, 2, 3, 6, or 12 h, and the cell survival rates were determined. Each bar represents a mean ± S.D. (n = 6). $^{**}P<0.01$ *vs* time 0, according to Dunnett's test. $^{\dagger}P<0.05$ between groups A and B, according to Student's *t*-test.

Discussion

This is the first report to reveal the precise temporal relationships between four reactions (mitochondrial depolarization, cyt.*c* release, caspase activation, and cellular shrinkage) in TNF-α-induced cell death. Because the onset of these reactions varied among individual cells, real-time single-cell imaging is the only currently available method to reveal temporal relationships between these reactions. We described our three-color real-time imaging technique in this report. Rehm et al. has reported the simultaneous real-time imaging of caspase activation and Smac release by using CFP/YFP-FRET sensor and YFP-tagged protein (26). They used the same color, YFP, for the observation of both reactions. It is possible to identify two reactions as they discussed, but it may be difficult to identify small changes occurring in the cell by their method. Previously, we revealed that DsRed was useful for FRET analysis of caspase activation (24). In this report, we observed caspase activation and cyt.*c* release with YFP/DsRed-FRET sensor and CFP-tagged protein. By using fluorescent probes in different colors, each reaction could be easily and precisely identified in a single cell.

We observed cell death at the single-cell level with a resolution period of 0.5 – 1 min, and we revealed that the relative timing between cyt.*c* release, caspase activation, and cellular shrinkage remained constant in all of the dying cells observed; however, the timing of mitochondrial depolarization showed a large deviation (Fig. 3). After cyt.*c* release, apoptosome formation, caspase-9 activation, caspase-3 activation, and the cleavage of various substrates that lead to apoptotic cell death are initiated. Our results revealed that this series of reactions takes place within 10 min and that the time course of this process was identical among all of the dying HeLa cells.

Mitochondrial depolarization was observed in all dying cells, but we considered that mitochondrial depolarization was not the cause of cyt.*c* release, caspase activation, and cellular shrinkage. Mitochondrial depolarization was found to occur at any time after cyt.*c* release. Mitochondrial depolarization was observed after caspase activation and cellular shrinkage in 60% of the observed cells. These results exclude the possibility that mitochondrial depolarization is a cause of cyt.*c* release, caspase activation, and/or cellular shrinkage. This is consistent with previous findings that cell death occurred without mitochondrial depolarization. Li et al. have shown that caspases are activated independently of mitochondrial depolarization in TNF-α-induced cell death (27). Krohn et al. have shown that cyt.*c* release and caspase activation occurred in the absence of mitochondrial depolarization in cell death of hippocampal neurons (28). Several studies suggested that mitochondrial depolarization is a critical step for cell death (29), but our results support the idea that mitochondrial depolarization is not crucial to the cell death process.

Cyt.*c* release may be a key step in two independent series of events, that is, the cell death process and mitochondrial depolarization. We speculate that cells might try to maintain cellular homeostasis by keeping membrane potential after cyt.*c* release. While maintaining the membrane potential, the released cyt.*c* immediately initiated the cell death process in the cytosol, and thus caspase activation and cellular shrinkage always took place within a short period of time. The timing of mitochondrial depolarization did not appear to be relevant to this process.

A number of imaging analyses have demonstrated that each cell death event is a rapid process. Initiator- and effector-caspase activation both proceed rapidly (23, 24, 30 – 32). Cyt.*c* is also released rapidly in a single step (33 – 35). Likewise, Smac/DIABLO is released rapidly, although the duration of Smac/DIABLO release is greater than that of cyt.*c* (26). Several multi-event imaging studies have suggested that cell death events occur almost simultaneously. Initiator caspase activation/effector caspase activation, effector caspase activation/mitochondrial depolarization, cyt.*c*/smac, and effector caspase activation/smac release had been analyzed simultaneously at the single-cell level and were found to occur almost simultaneously (24, 26). These findings, taken together with our present results, suggest that the cell death cascade proceeds rapidly after mitochondrial changes take place.

Once cyt.*c* was released, the following reactions proceed in a rapid manner. However, it did take 253.4 ± 92.5 min from TNF-α treatment to cyt.*c* release, and this duration varied from cell to cell (Figs. 3 and 4). We observed some cells that had died within 1 h in imaging analysis, indicating that cells have the ability to induce cell death within 1 h, and suggesting that certain factors may delay signal transduction and the timing of cell death. The results shown in Fig. 4 indicate that these factors were active only when the cells were exposed to TNF-α. We considered two possible explanations for these findings. 1: Each TNF-α molecule changed the cell slightly, and the changes induced by one molecule were not sufficient to induce the cell death cascade on their own. However, many TNF-α molecules attacked the cell, and intracellular changes thus accumulated. When the accumulated changes exceeded the threshold level, the cell death cascade would be expected to have proceeded rapidly. 2: TNF-α could induce intracellular changes by chance. According to this explanation, TNF-α molecules would bind with the TNF receptor, but only some of them would be able to induce intracellular change. If some TNF-α molecules successfully induce intracellular changes, then the cell death cascade would proceed rapidly. The more TNF-α molecules that are present around the cell, and/or the longer these TNF-α molecules attack the cell, the higher the probability of a successful attack, and it can be expected that more cells will die. According to both of these models, the cell death process would not proceed in the absence of TNF-α exposure; therefore, those cells that survived during TNF-α exposure would not be expected to die after the removal of TNF-α.

One of the Bcl-2 family proteins, Bid, was cleaved to tBid due to the cell death signal, and the tBid transferred the signal from the cytosol to the mitochondria (36). Exogenous treatment with tBid is known to induce cell death immediately (37), and thus reactions that delay signal transduction may occur at an earlier step than either Bid cleavage or mitochondrial changes.

As cell death reactions often occur in a rapid manner and because the timing of the onset of intracellular reactions varies among cells, precise temporal relationships between cellular events during cell death should be further analyzed at the single-cell level with high temporal resolution. Single-cell imaging analyses of early stages (e.g., receptor oligomerization and the recruitment of adaptor proteins) will help to elucidate the mechanism of the entire cell death process.

Acknowledgments

This study was supported in part by a Grant-in-Aid for Research on Health Sciences focusing on Drug Innovation from the Japan Health Science Foundation; a Grant-in-Aid for Research on Advanced Medical Technology from the Ministry of Health, Labour, and Welfare; and a grant (MF-16) from the Organization for Pharmaceutical Safety and Research.

References

1 Thornberry NA, Lazebnik Y. Caspases: enemies within. Science. 1998;281:1312–1316.

2 Stennicke HR, Salvesen GS. Properties of caspases. Biochim Biophys Acta. 1998;1387:17–31.

3 Boldin MP, Goncharov TM, Goltsev YV, Wallach D. Involvement of MACH, a novel MORT1/FADD-interacting protease, in Fas/APO-1- and TNF receptor-induced cell death. Cell. 1996; 85:803–815.

4 Muzio M, Chinnaiyan AM, Kischkell FC, O'Rourke K, Shevchenko A, Ni J, et al. FLICE, a novel FADD-homologous ICE/CED-3-like protease, is recruited to the CD95 (Fas/APO-1) death-inducing signal complex. Cell. 1996;85:817–827.

5 Medema JP, Scaffidi C, Kischkel FC, Shevchenko A, Mann M, Krammer PH, et al. FLICE is activated by association with the CD95 death-inducing signaling complex (DISC). EMBO J. 1997;16:2794–2804.

6 Martin DA, Siegel RM, Zheng L, Lenardo MJ. Membrane oligomerization and cleavage activates the caspase-8 (FLICE /MACHalpha1) death signal. J Biol Chem. 1998;273:4345–4349.

7 Srinivasula SM, Ahmad M, Fernandes-Alnemri T, Litwack G, Alnemri ES. Molecular ordering of the Fas-apoptotic pathway: The Fas/APO-1 protease Mch5 is a CrmA-inhibitable protease that activates multiple Ced-3/ICE-like cysteine proteases. Proc Natl Acad Sci U S A. 1996;93:14486–14491.

8 Orth K, O'Rourke K, Salvesen GS, Dixit VM. Molecular ordering of apoptotic mammalian CED-3/ICE-like proteases. J Biol Chem. 1996;271:20977–20980.

9 Tewari M, Quan LT, O'Rourke K, Desnoyers S, Zeng Z, Beidler DR, et al. Yama/CPP32 beta, a mammalian homolog of CED-3, is a CrmA-inhibitable protease that cleaves the death substrate poly(ADP-ribose) polymerase. Cell. 1995;81:801–809.

10 Green DR, Reed JC. Mitochondria and apoptosis. Science. 1998;281:1309–1312.

11 Martinou JC, Green DR. Breaking the mitochondrial barrier. Nat Rev Mol Cell Biol. 2001;2:63–67.

12 Saleh A, Srinivasula SM, Acharya S, Fishel R, Alnemri ES. Cytochrome c and dATP-mediated oligomerization of Apaf-1 is a prerequisite for procaspase-9 activation. J Biol Chem. 1999;274:17941–17945.

13 Shiozaki EN, Chai J, Shi Y. Oligomerization and activation of caspase-9, induced by Apaf-1 CARD. Proc Natl Acad Sci U S A. 2002;99:4197–4202.

14 Tyas L, Brophy VA, Pope A, Rivett AJ, Tavare JM. Rapid caspase-3 activation during apoptosis revealed using fluorescence-resonance energy transfer. EMBO reports. 2000;1:266–270.

15 Rehm M, Dussmann H, Janicke RU, Tavare JM, Kogel D, Prehn JHM. Single-cell fluorescence resonance energy transfer analysis demonstrates that caspase activation during apoptosis is a rapid process: role of caspase-3. J Biol Chem. 2002;277: 24506–24514.

16 Luo KQ, Yu VC, Pu Y, Chang DC. Application of the fluorescence resonance energy transfer method for studying the dynamics of caspase-3 activation during UV-induced apoptosis in living HeLa cells. Biochem Biophys Res Commun. 2001;283:1054–1060.

17 Morgan MJ, Thorburn A. Measurement of caspase activity in individual cells reveals differences in the kinetics of caspase activation between cells. Cell Death Differ. 2001;8:38–43.

18 Tsien RY, Miyawaki A. Seeing the machinery of live cells. Science. 1998;280:1954–1955.

19 Miyawaki A, Sawano A, Kogure T. Lighting up cells: labeling proteins with fluorophores. Nat Cell Biol. 2003;S1–S7.

20 Tsien RY, The green fluorescent protein. Annu Rev Biochem. 1998;67:509–544.

21 Erickson MG, Moon DL, Yue DT. DsRed as a potential FRET partner with CFP and GFP. Biophys J. 2003;85:599–611.

22 Karasawa S, Araki T, Nagai T, Mizuno H, Miyawaki A. Cyan-emitting and orange-emitting fluorescent proteins as a donor

/acceptor pair for fluorescence resonance energy transfer. Biochem J. 2004;381:307–312.

23 Kawai H, Suzuki T, Kobayashi T, Mizuguchi H, Hayakawa T, Kawanishi T. Simultaneous imaging of initiator/effector caspase activity and mitochondrial membrane potential during cell death in living HeLa cells. Biochim Biophys Acta. 2004;1693:101–110.

24 Kawai H, Suzuki T, Kobayashi T, Sakurai H, Ohata H, Honda K, et al. Simultaneous real-time detection of initiator- and effector-caspase activation by double fluorescence resonance energy transfer analysis. J Pharmacol Sci. 2005;97:361–368.

25 Scaduto RC Jr, Grotyohann LW. Measurement of mitochondrial membrane potential using fluorescent rhodamine derivatives. Biophys J. 1999;76:469–477.

26 Rehm M, Dussmann H, Prehn JHM. Real-time single cell analysis of Smac/DIABLO release during apoptosis. J Cell Biol. 2003;162:1031–1043.

27 Li X, Du L, Darzynkiewicz Z. During apoptosis of HL-60 and U-937 cells caspases are activated independently of dissipation of mitochondrial electrochemical potential. Exp Cell Res. 2000;257:290–297.

28 Krohn AJ, Wahlbrink T, Prehn JHM. Mitochondrial depolarization is not required for neuronal apoptosis. J Neurosci. 1999;19:7394–7404.

29 Heiskanen KM, Bhat MB, Wang H-W, Ma J, Nieminen A-L. Mitochondrial depolarization accompanies cytochrome c release during apoptosis in PC6 cells. J Biol Chem. 1999;274:5654–5658.

30 Ohnuki R, Nagasaki A, Kawasaki H, Baba T, Uyeda TQP, Taira K. Confirmation by FRET in individual living cells of the absence of significant amyloid β-mediated caspase 8 activation. Proc Natl Acad Sci U S A. 2002;99:14716–14721.

31 Takemoto K, Nagai T, Miyawaki A, Miura M. Spatio-temporal activation of caspase revealed by indicator that is insensitive to environmental effects. J Cell Biol. 2003;160:235–243.

32 Luo KQ, Yu VC, Pu Y, Chang DC. Measuring dynamics of caspase-8 activation in a single living HeLa cell during TNFalpha-induced apoptosis. Biochem Biophys Res Commun. 2003;304:217–222.

33 Lim MLR, Lum M-G, Hansen TM, Roucou X, Nagley P. On the release of cytochrome c from mitochondria during cell death signaling. J Biomed Sci. 2002;9:488–506.

34 Goldstein JC, Waterhouse NJ, Juin P, Evan GI, Green DR. The coordinate release of cytochrome c during apoptosis is rapid, complete and kinetically invariant. Nat Cell Biol. 2000;2:156–162.

35 Goldstein JC, Munoz-Pinedo C, Ricci J-E, Adams SR, Kelekar A, Schuler M, et al. Cytochrome c is released in a single step during apoptosis. Cell Death Differ. 2005;12:453–462.

36 Luo X, Budihardjo I, Zou H, Slaughter C, Wang X. Bid, a Bcl-2 interacting protein, mediates cytochrome c release from mitochondria in response to activation of cell surface death receptors. Cell. 1998;94:481–490.

37 Madesh M, Antonsson B, Srinivasula SM, Alnemri ES, Hajnóczky G. Rapid kinetics of tbid-induced cytochrome *c* and Smac/DIABLO release and mitochondrial depolarization. J Biol Chem. 2002;277:5651–5659.